Physics Letters B 759 (2016) 9–35

Contents lists available at ScienceDirect

Physics Letters B

www.elsevier.com/locate/physletb

Search for supersymmetry in events with soft leptons, low jet multiplicity, and missing transverse energy in proton–proton collisions at $\sqrt{s} = 8$ TeV

CMS Collaboration *

CERN, Switzerland

ARTICLE INFO

Article history:
Received 25 December 2015
Received in revised form 7 April 2016
Accepted 11 May 2016
Available online 16 May 2016
Editor: M. Doser

Keywords:
CMS
Physics
Supersymmetry

ABSTRACT

Results are presented from a search for supersymmetric particles in scenarios with small mass splittings. The data sample corresponds to 19.7 fb^{-1} of proton–proton collisions recorded by the CMS experiment at $\sqrt{s} = 8$ TeV. The search targets top squark ($\tilde{\mathrm{t}}$) pair production in scenarios with mass differences $\Delta m = m(\tilde{\mathrm{t}}) - m(\tilde{\chi}_1^0)$ below the W-boson mass and with top-squark decays in the four-body mode ($\tilde{\mathrm{t}} \to \mathrm{b}\ell\nu\tilde{\chi}_1^0$), where the neutralino ($\tilde{\chi}_1^0$) is assumed to be the lightest supersymmetric particle (LSP). The signature includes a high transverse momentum (p_{T}) jet associated with initial-state radiation, one or two low-p_{T} leptons, and significant missing transverse energy. The event yields observed in data are consistent with the expected background contributions from standard model processes. Limits are set on the cross section for top squark pair production as a function of the $\tilde{\mathrm{t}}$ and LSP masses. Assuming a 100% branching fraction for the four-body decay mode, top-squark masses below 316 GeV are excluded for $\Delta m = 25$ GeV at 95% CL. The dilepton data are also interpreted under the assumption of chargino–neutralino production, with subsequent decays to sleptons or sneutrinos. Assuming a difference between the common $\tilde{\chi}_1^+/\tilde{\chi}_2^0$ mass and the LSP mass of 20 GeV and a τ-enriched decay scenario, masses in the range $m(\tilde{\chi}_1^+) < 307$ GeV are excluded at 95% CL.

© 2016 The Author. Published by Elsevier B.V. This is an open access article under the CC BY license (http://creativecommons.org/licenses/by/4.0/). Funded by SCOAP[3].

1. Introduction

The main objectives of the CERN LHC programme include searches for new physics, in particular supersymmetry (SUSY) [1–5], one of the most promising extensions of the standard model (SM) of particle physics. Supersymmetric models can offer solutions to several shortcomings of the SM, in particular those related to the mass hierarchy of elementary particles [6,7] and to the presence of dark matter in the universe.

Supersymmetry predicts superpartners of SM particles (sparticles) whose spins differ by one-half unit with respect to their SM partners. In SUSY models with R-parity [8] conservation, sparticles are pair-produced and their decay chains end with the lightest supersymmetric particle (LSP). In many of these models the lightest neutralino ($\tilde{\chi}_1^0$) takes the role of the LSP and, being neutral and weakly interacting, would match the characteristics required of a dark matter candidate. The LSPs would remain undetected and yield a characteristic signature of high missing transverse momentum, the magnitude of which is referred to as $E_{\mathrm{T}}^{\mathrm{miss}}$.

In this paper we investigate the production of supersymmetric particles in a scenario in which the mass splitting between the next-to-lightest SUSY particle (NLSP) and the LSP is small, which is referred to as compressed SUSY. In this case, the events would escape classical search strategies because of the low transverse momenta (p_{T}) of the decay products of the NLSP. Signal events can still be distinguished from SM processes if a high-p_{T} jet from initial-state radiation (ISR) leads to a boost of the sparticle pair system and enhances the amount of $E_{\mathrm{T}}^{\mathrm{miss}}$, while the other decay products typically remain soft. In the signal scenarios studied in this paper, SUSY particles can decay leptonically, and the presence of low-p_{T} leptons can be used to discriminate further against otherwise dominant SM backgrounds, such as multijet production and Z + jets events with invisible Z boson decays.

SUSY models with light top squarks ($\tilde{\mathrm{t}}$) are well motivated as they control the dominant correction to the Higgs boson mass and thereby preserve "naturalness" [6,7,9–14]. SUSY scenarios with mass splittings of 15–30 GeV between the top squark and the LSP

* *E-mail address:* cms-publication-committee-chair@cern.ch.

http://dx.doi.org/10.1016/j.physletb.2016.05.033
0370-2693/© 2016 The Author. Published by Elsevier B.V. This is an open access article under the CC BY license (http://creativecommons.org/licenses/by/4.0/). Funded by SCOAP[3].

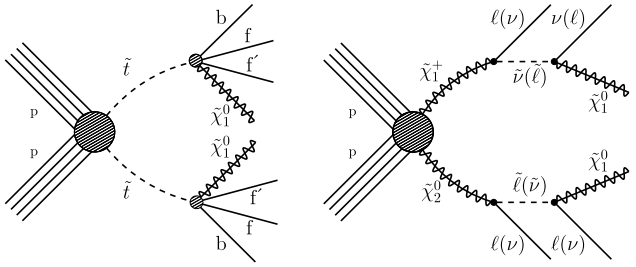

Fig. 1. Signal models for top squark pair production with subsequent four-body decays (left), and chargino–neutralino pair production with decays via sleptons and sneutrinos (right). Antiparticle labels are suppressed. The ISR jet used in the analysis is not shown in these diagrams.

are especially interesting because they would lead, through $\tilde{t}$–$\tilde{\chi}_1^0$ co-annihilation, to the observed cosmological abundance of dark matter [15]. For mass differences below the W-boson mass, top squarks could undergo either a two-body decay (such as $\tilde{t} \to c\tilde{\chi}_1^0$) or a four-body decay ($\tilde{t} \to bff'\tilde{\chi}_1^0$, where ff′ represents a pair of quarks or leptons), as shown in the left panel of Fig. 1, with branching fractions and kinematic properties that depend on details of the model [16,17]. The search strategy based on the presence of an ISR jet has been used to search for the two-body decay in a monojet topology by the CMS Collaboration [18], and for both decay modes by the ATLAS Collaboration [19–21]. In this paper we assume that other SUSY particles are decoupled and that the four-body decay proceeds exclusively via virtual SM particles.

Final states with a hard ISR jet, high $E_{\mathrm{T}}^{\mathrm{miss}}$, and one or more charged leptons can also occur in the production of chargino–neutralino pairs in compressed SUSY models [22–24]. A model of pair-production of the lightest chargino ($\tilde{\chi}_1^+$) with the second-lightest neutralino ($\tilde{\chi}_2^0$) is shown in Fig. 1 (right). Decay chains could proceed via intermediate sleptons or sneutrinos and give rise to final states with one or three charged leptons. In this model, $\tilde{\chi}_1^+$ and $\tilde{\chi}_2^0$ are assumed to be almost degenerate and are assigned a common mass $m(\tilde{\chi})$. In general, the same signature can arise from the production of heavy particles whose decay chains contain undetected, slightly lighter particles plus leptons. Previous LHC results for the model of electroweak production described above and mass splittings below $m(\mathrm{Z})$ can be found in Refs. [25–29], where the last two references also report an alternative approach based on the vector-boson fusion topology.

In this paper we describe a search for pair production of top squarks with subsequent four-body decays via virtual top quarks and W bosons in events with a high-p_{T} jet, $E_{\mathrm{T}}^{\mathrm{miss}}$, and one or two soft leptons, corresponding to signal events with a leptonic decay of at least one of the virtual W bosons. The single-lepton topology offers the second-highest branching fraction after the purely hadronic mode. In this channel we consider only muons, which can be efficiently reconstructed and identified with transverse momenta as low as 5 GeV. For the dilepton topology we require a second lepton (electron or muon) of opposite charge. The single and double electron final states are not used because they have reduced sensitivity compared to the muon channels due to the higher p_{T} thresholds required for electrons. In addition, selected events are required to have an energetic jet compatible with the ISR signature, at most one additional jet of moderate to high p_{T}, no hard leptons, and a significant amount of $E_{\mathrm{T}}^{\mathrm{miss}}$. The dominant SM backgrounds to this search are pair production of top quarks, W boson or Z/γ^* production in association with jets, and diboson (VV) production. Their contributions to the signal region (SR) are estimated by correcting the predictions from simulation using the event yields observed in several control regions (CRs) in data. Data are also used to validate this procedure and to derive systematic uncertainties.

The results of the dilepton search are also interpreted in terms of the model of $\tilde{\chi}_1^+$–$\tilde{\chi}_2^0$ pair production discussed above. For small $\tilde{\chi}_1^+ - \tilde{\chi}_1^0$ mass splittings, the leptons in the final state would be soft and therefore within the signal region of the dilepton search.

2. Detector description and event reconstruction

The CMS detector has been described in detail in Ref. [30]. Its central feature is a superconducting solenoid that provides a homogeneous field of 3.8 T in a volume containing a silicon pixel and strip tracker, a lead tungstate crystal electromagnetic calorimeter, and a brass and scintillator hadron calorimeter. Muons are measured in gas-ionization chambers embedded in the steel flux-return yoke surrounding the solenoid. The acceptance of the silicon tracker and the muon systems extends to pseudorapidities of $|\eta| < 2.5$ and < 2.4, respectively. The barrel and endcap calorimeters cover the range $|\eta| < 3.0$ and are complemented by extensive forward calorimetry. Events are selected for further analysis by a two-tier trigger system that uses custom hardware processors to make a fast initial selection, followed by a more detailed selection executed on a dedicated processor farm.

The measurement of jets and $E_{\mathrm{T}}^{\mathrm{miss}}$ is based on candidates reconstructed by the particle-flow (PF) algorithm [31,32], which identifies leptons, photons, and charged and neutral hadrons by combining information from all subdetectors. The PF candidates are clustered into jets by using the anti-k_{T} algorithm [33] with a distance parameter of 0.5. Jets are required to have $p_{\mathrm{T}} > 30$ GeV and $|\eta| < 4.5$, and to pass loose quality criteria [34] based on the energy fractions associated with electromagnetically or hadronically interacting charged or neutral particles. The negative vector sum of the transverse momenta of the PF candidates defines the value of $E_{\mathrm{T}}^{\mathrm{miss}}$ and the corresponding direction. Jet energies and $E_{\mathrm{T}}^{\mathrm{miss}}$ are corrected for shifts in the energy scale, contributions from additional, simultaneous proton–proton collisions (pileup), and residual differences between data and simulation [35,36]. Jets originating from b quarks are identified ("tagged") using the combined secondary vertex algorithm [37,38] at a working point corresponding to an efficiency of about 70% and a misidentification probability for light-quark jets of about 1%. Hadronic decays of τ leptons are identified using the hadrons-plus-strips algorithm [39].

Muons and electrons are required to have p_{T} above 5 and 7 GeV, respectively. In the single-muon search, the lepton acceptance is restricted to $|\eta| < 2.1$, while in the dilepton search, this limit is tightened to 1.5 for both electrons and muons. Standard loose identification requirements [40,41] are applied to reduce the background from nonprompt (NPR) leptons produced in semileptonic hadron decays and from jets showing a lepton signature. Further background reduction is achieved by requiring the leptons to be isolated. The absolute isolation I_{abs} is computed by summing the transverse momenta of PF candidates, except that of the lepton, in a cone of size $\Delta R < 0.3$ around the lepton direction, where $\Delta R \equiv \sqrt{(\Delta\phi)^2 + (\Delta\eta)^2}$ and ϕ is the azimuthal angle measured in radians. The energy in the isolation cone is corrected for the effects of pileup. The relative isolation I_{rel} is obtained by dividing I_{abs} by the p_{T} of the lepton. The details of the isolation requirements differ between the single-lepton and dilepton topologies due to differences in the dominant backgrounds and the purities. They are described in Sections 4 and 5.

3. Samples and event preselection

The data sample comprises proton–proton collisions recorded in 2012 at a centre-of-mass energy of 8 TeV and corresponds to an

integrated luminosity of 19.7 fb^{-1}. The search uses events passing one of several online $E_{\mathrm{T}}^{\mathrm{miss}}$ selections. These triggers evolved over the data-taking period and required either $E_{\mathrm{T}}^{\mathrm{miss}} > 120$ GeV, where $E_{\mathrm{T}}^{\mathrm{miss}}$ is reconstructed from the energy deposited in the calorimeters, or $E_{\mathrm{T}}^{\mathrm{miss}} > 95$ GeV and a jet with $p_{\mathrm{T}} > 80$ GeV and $|\eta| < 2.6$, where both objects are reconstructed using the PF algorithm. In the second part of the data-taking period, the threshold on $E_{\mathrm{T}}^{\mathrm{miss}}$ was raised from 95 to 105 GeV. Control samples were collected based on a single-muon trigger with a p_{T} threshold of 24 GeV.

Simulated Monte Carlo (MC) samples of SM background events are produced by using several generators. Single and pair production of top quarks are simulated by using the POWHEG 1.0 [42] program. Simulations of multijet and diboson events are done with PYTHIA 6.4 [43]. The generation of all other relevant samples, in particular Z/γ^* processes, $\mathrm{W}+$ jets events, and $\mathrm{t\bar{t}}$ production in association with a W, Z, or Higgs boson, is performed with the MADGRAPH 5.1 [44] generator. Alternative samples of $\mathrm{t\bar{t}}$ and diboson events are also produced using MADGRAPH to investigate possible systematic differences, which are found to be insignificant in the context of the analyses described in this paper. All samples generated with MADGRAPH or POWHEG are passed to PYTHIA 6.4 with the Z2* tune [45] for hadronization and showering. The detector response is simulated with the GEANT4 [46] program. Finally, all events are reconstructed with the same algorithms as the ones used for data. Pileup events are included in the simulation and all samples are reweighted to match the distribution of the average number of these events in data.

The signal simulation for $\tilde{\mathrm{t}}$ pair production is done on a grid in the $\tilde{\mathrm{t}}$–$\tilde{\chi}_1^0$ mass plane with $m(\tilde{\mathrm{t}})$ ranging from 100–400 GeV in steps of 25 GeV, and $\Delta m \equiv m(\tilde{\mathrm{t}}) - m(\tilde{\chi}_1^0)$ ranging from 10–80 GeV in steps of 10 GeV. The production of top-squark pairs with up to two additional jets and the four-body decays of the top squarks are generated with MADGRAPH. The decays are forced to proceed only through virtual SM particles. Chargino–neutralino pair production is also modelled with MADGRAPH, while their decays are generated with PYTHIA. We assume a bino-like LSP and wino-like $\tilde{\chi}_2^0$ and $\tilde{\chi}_1^+$ in order to allow a direct comparison with Ref. [25]. A range in the common gaugino mass of 100–400 GeV is covered with steps of 20 GeV, maintaining a fixed mass difference of 20 GeV above the $\tilde{\chi}_1^0$. As for the background samples, the generation steps for both signal models are followed by hadronization and showering in PYTHIA. For the signal samples, the modelling of the detector response is performed with the CMS fast simulation program [47]. Differences in the efficiencies of the lepton selection and the b-jet identification between the fast and the detailed GEANT4 simulation are corrected by using scale factors. Deficiencies in the modelling of ISR in the simulation [48] are corrected by applying a weight as a function of the p_{T} of the recoiling system.

The effects of residual differences between data and simulation are taken into account in the analysis. The systematic uncertainty related to possible variations in the jet energy scale [35] is evaluated by a coherent change of all jet energies, which is also propagated to $E_{\mathrm{T}}^{\mathrm{miss}}$. The jet energy resolution in simulation is found to be slightly better than in data [35]. To compensate for this effect, the energies of simulated jets are smeared and a corresponding systematic uncertainty is assigned. Simulation is corrected for differences in the efficiencies of the reconstruction of leptons, and of the identification of leptons [40,41] and b jets [37,38] with respect to the values measured in data. The corresponding uncertainties are propagated to the final results.

The first step in the event selection is designed to match the online requirements and to serve as a common basis for the analysis in both channels. It is guided by the general characteristics of signal events. The leading jet of each event is considered as an ISR jet candidate. It is required to pass tighter jet identification criteria and to fulfil $p_{\mathrm{T}} > 110$ GeV and $|\eta| < 2.4$. Since jets resulting from $\tilde{\mathrm{t}}$ decays are soft, and no jets are expected from $\tilde{\chi}_2^0$ or $\tilde{\chi}_1^+$ decays, at most one additional jet with $p_{\mathrm{T}} > 60$ GeV is accepted. At least one identified muon with $p_{\mathrm{T}} > 5$ GeV and $|\eta| < 2.1$ must be present. Finally, a requirement of $E_{\mathrm{T}}^{\mathrm{miss}} > 200$ GeV is imposed. By using a control sample collected with the single-muon trigger, the signal triggers are found to be fully efficient after these preselection criteria are applied.

4. Search in the single-lepton channel

The single-lepton topology is selected by requiring at least one muon within the acceptance described in the previous sections. Events are rejected if an electron, a τ lepton, or an additional muon with $p_{\mathrm{T}} > 20$ GeV is present. To avoid strong variations of the muon selection efficiency with p_{T}, a combined isolation criterion, $I_{\mathrm{abs}} < 5$ GeV or $I_{\mathrm{rel}} < 0.2$, is used, equivalent to a transition from an absolute to a relative isolation requirement at $p_{\mathrm{T}} = 25$ GeV. The impact parameters of the muon with respect to the primary collision vertex in the transverse plane, d_{xy}, and longitudinal direction, d_{z}, are required to be smaller than 0.02 and 0.5 cm, respectively. The primary vertex is chosen as the one with the highest sum of ${p_{\mathrm{T}}}^2$ of its associated tracks. Furthermore, requirements are imposed on $E_{\mathrm{T}}^{\mathrm{miss}}$ and on the scalar sum of the transverse momenta of all jets, H_{T}. Since these two observables are correlated, a simultaneous selection is applied by using the combined variable $C_{\mathrm{T}} \equiv \min(E_{\mathrm{T}}^{\mathrm{miss}}, H_{\mathrm{T}} - 100\ \mathrm{GeV})$. To match the preselection, $C_{\mathrm{T}} > 200$ GeV is required. Background from SM dijet and multijet production is suppressed by requiring the azimuthal angle between the momentum vectors of the two leading jets to be smaller than 2.5 rad for all events with a second hard jet of $p_{\mathrm{T}} > 60$ GeV. According to simulation, the remaining sample is dominated by $\mathrm{W}+$ jets and, to a lesser extent, by $\mathrm{t\bar{t}}$ production with a single prompt lepton in the final state. Therefore, we use the transverse mass m_{T} [49] computed from the transverse components of the muon momentum and the $E_{\mathrm{T}}^{\mathrm{miss}}$ vector as a discriminant.

Distributions of the muon p_{T} and of m_{T} at this stage of the selection are presented in Fig. 2. They show good agreement between data and simulation. The variation of the signal shapes is illustrated with two extreme cases of the mass splitting (10 and 80 GeV).

To maintain sensitivity over a large range of Δm values, several SRs are defined as listed in Table 1. Since signal leptons have low p_{T}, we impose an upper limit of $p_{\mathrm{T}} < 30$ GeV in all these selections. Because the muon p_{T} spectrum of the signal changes rapidly with Δm, the full range of muon p_{T} is subdivided into three bins in the calculation of the final results: 5–12, 12–20, and 20–30 GeV.

The signal region labelled as SRSL1 is designed for low values of Δm, where the b jets produced in the $\tilde{\mathrm{t}}$ decays rarely pass the selection thresholds. A veto on b-tagged jets strongly reduces the contribution from $\mathrm{t\bar{t}}$ events. In addition, only events with negatively charged muons ($Q = -1$) are accepted, using the fact that the remaining $\mathrm{W}+$ jets background shows significantly more positively than negatively charged muons [50] while the signal is symmetric in the muon charge. The acceptance for muons is reduced to the central region, $|\eta| < 1.5$, and the requirement on C_{T} is tightened to 300 GeV. For signal points at low Δm, m_{T} is typically small, mainly due to the soft lepton p_{T} spectrum. With increasing Δm, the average m_{T} increases and eventually the distribution extends to values above $m(\mathrm{W})$. To cover the full range of Δm values, SRSL1 is therefore divided into three subregions, SRSL1a–c,

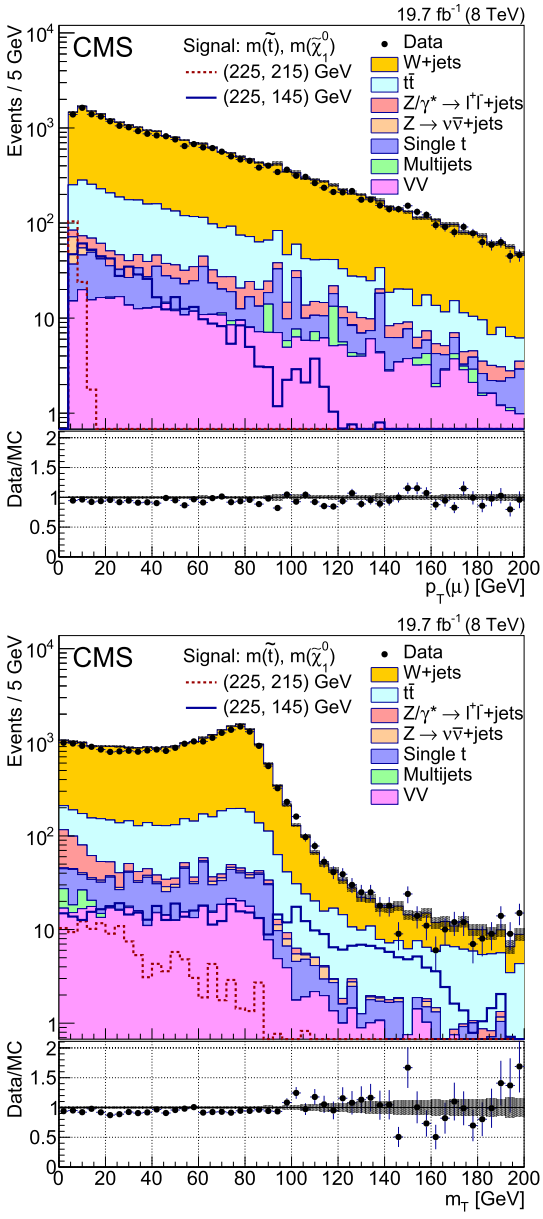

Fig. 2. Distributions of (top) muon p_T and (bottom) m_T after the preselection of the single-muon analysis. For each plot, the variable shown has been excluded from the selection. Data are indicated by circles. The uncorrected background predictions from simulation are represented as filled, stacked histograms, and the shapes for two signal points with $m(\tilde{t}) = 225$ GeV and mass splittings of $\Delta m = 10$ and 80 GeV as dashed red and solid blue lines, respectively. The error bars and the dark, shaded bands indicate the statistical uncertainties of data and simulation, respectively. The lower panels show the ratio of data to the sum of the SM backgrounds. (For interpretation of the references to colour in this figure legend, the reader is referred to the web version of this article.)

defined by $m_T < 60$ GeV, $60 < m_T < 88$ GeV, and $m_T > 88$ GeV, respectively.

The second signal region (SRSL2) targets signals with higher mass splitting, where some of the b jets enter the acceptance. Therefore, the b jet veto in the region $30 < p_T < 60$ GeV is reversed, and at least one such jet is required. Events with one or more b-tagged jets with $p_T > 60$ GeV are still rejected to reduce the $t\bar{t}$ background. In addition, the p_T threshold of the ISR jet candidate is raised to 325 GeV. This second SR receives a strong contribution from $t\bar{t}$ events.

4.1. Background estimation

The following four background contributions are estimated by using data: W + jets and $t\bar{t}$ production, which are the dominant components for the single-muon search; $(Z \to \nu\nu)$ + jets, which is relevant for a signal region at high m_T as explained below; and multijet production. For the first three of these backgrounds, data/simulation scale factors are determined in suitable CRs and applied to the simulated yields in the SR. The contribution of multijet events is estimated by using data only. Rare backgrounds (other Z/γ^* processes, and diboson and single top quark production) are predicted by using simulation.

Simulation provides only an imperfect description of the p_T spectrum for the main background samples (W + jets, $t\bar{t}$). Since the extrapolations from control to signal regions involve the lepton p_T spectrum, the p_T distributions of W bosons (for W + jets events) and top quarks (for $t\bar{t}$ events) are corrected based on measurements in data samples dominated by $t\bar{t}$, Z + jets, and W + jets events before deriving the scale factors.

For the estimation of the $t\bar{t}$ background, a single control region (CRSL($t\bar{t}$)) is used: events are required to pass the basic selection defined above and must include at least two b-tagged jets, with one of them in the p_T region above 60 GeV. This CR has an estimated purity of 80% in $t\bar{t}$ events. The observed event count in CRSL($t\bar{t}$) is corrected for other background contributions and compared to the yield estimated from $t\bar{t}$ simulation. The resulting scale factor of 1.05 is then used to modify the predictions of the $t\bar{t}$ simulation in all SRs.

The W + jets yields from simulation are normalized in control regions associated to each of the four signal (sub-)regions SRSL1a–c (CRSL1a–c) and SRSL2 (CRSL2). Control and signal regions differ only by the muon p_T range: in the CRs a muon with $p_T > 30$ GeV is required. The control regions CRSL1a–c have an estimated purity of 80% in W + jets events. For region CRSL2 this number is about 50%, the remainder being dominated by $t\bar{t}$ events. Again, scale factors are derived after subtracting non-W + jets backgrounds from the observed yields in the CR. The $t\bar{t}$ yields used in the subtraction are corrected by the scale factor determined as described in the previous paragraph. The scale factors for W + jets simulation vary from 0.88–1.18 in the four signal regions SRSL1a–c and SRSL2.

Each factor is applied to all three muon p_T bins of a signal region. Systematic uncertainties are assigned related to the statistical uncertainties of the factors (6–30%), and to the shape of the p_T spectrum as described later in this section. The definitions of the single-lepton signal and control regions are summarized in Table 1, and the expected compositions of the events in the control regions are shown in Table 2. For the benchmark signal models, the control regions would typically receive a contribution from signal events at the level of a few percent. This effect is taken into account in the statistical analysis of the results.

After applying the signal selection, with the exception of the requirement on muon p_T, the muon p_T spectra of $t\bar{t}$ and W + jets events are similar. Therefore, the correction procedure leads to an anti-correlation of the estimates for the two categories and a relative uncertainty in the sum of the two contributions that is smaller than the uncertainty in a single component. For this reason, the analysis is robust against variations in the relative yields of $t\bar{t}$ and W + jets events: a validation based on the direct estimation of the sum of both background components from the control regions CRSL1a–c and CRSL2 yields almost identical results in terms of the total background. The anti-correlation between the two backgrounds is taken into account in the computation of the results described in Section 6.

Table 1
Definition of signal and control regions for the single-muon search. For jets, the attributes "soft" and "hard" refer to the p_T ranges 30–60 GeV and > 60 GeV, respectively. For the calculation of the final results, each signal region (SRSL1a–c, SRSL2) is subdivided into three bins according to $p_T(\mu)$: 5–12, 12–20, and 20–30 GeV.

Variable	SRSL1a–c, CRSL1a–c	SRSL2, CRSL2	CRSL($t\bar{t}$)
E_T^{miss} (GeV)	> 300	> 300	> 200
H_T (GeV)	> 400	–	> 300
p_T(ISR jet) (GeV)	> 110	> 325	> 110
Number of hard jets	≤ 2	≤ 2	≤ 2
$\Delta\phi$(hard jets) (rad)	< 2.5	< 2.5	< 2.5
Number of b jets	0	≥ 1 soft 0 hard	(≥ 1 soft and ≥ 1 hard) or (≥ 2 hard)
$p_T(\mu)$ (GeV)	5–30 (SR), > 30 (CR)	5–30 (SR), > 30 (CR)	> 5
$\lvert\eta(\mu)\rvert$	< 1.5	< 2.4	< 2.4
$d_{xy}(\mu)$ (cm)	< 0.02	< 0.02	< 0.02
$d_z(\mu)$ (cm)	< 0.5	< 0.5	< 0.5
$Q(\mu)$	-1	any	any
Lepton rejection	no e, τ, or additional μ with $p_T > 20$ GeV		
m_T (GeV)	< 60 (a), 60–88 (b), > 88 (c)	–	–

Table 2
Contributions to the control regions of the single-muon analysis as determined from simulation before application of scale factors, together with the observed event counts. All uncertainties are statistical.

Background	CRSL($t\bar{t}$)	CRSL1a	CRSL1b	CRSL1c	CRSL2
W + jets	67.9 ± 3.6	323.3 ± 6.4	141.9 ± 4.3	30.3 ± 2.0	36.5 ± 2.3
$t\bar{t}$	471.0 ± 9.6	19.5 ± 2.2	9.9 ± 1.5	6.1 ± 1.2	37.5 ± 3.5
$Z/\gamma^* +$ jets	2.1 ± 0.5	16.1 ± 1.0	0.8 ± 0.2	0.3 ± 0.1	0.7 ± 0.2
VV	3.8 ± 0.6	13.7 ± 1.3	8.0 ± 1.1	2.5 ± 0.5	1.1 ± 0.4
Single top quark	58.6 ± 12.6	4.6 ± 1.4	3.3 ± 1.2	1.1 ± 0.7	3.5 ± 1.2
Total SM	603.4 ± 16.2	377.1 ± 7.1	165.0 ± 4.8	40.3 ± 2.5	79.4 ± 4.3
Data	628	347	172	46	75

The extrapolation of the correction factors from control to signal regions has been validated by comparing corrected yields from simulation to data in sideband regions. Each of these sidebands is defined by one of the following changes with respect to the signal selection: (a) a lowering of the E_T^{miss}/H_T requirement to $200 < C_T < 300$ GeV, (b) a change in the muon charge requirement, and (c) the condition of exactly one b-tagged jet with $p_T > 60$ GeV. The predictions in the sidebands are compatible with the observations, and the results are used to assign systematic uncertainties on the extrapolation of the scale factors to the SRs. These uncertainties are 20% for the estimate of the $t\bar{t}$ background and 10–30% for the estimate of the W + jets background where the highest uncertainty applies to region SRL1c.

At high values of m_T, only a few W + jets events pass the SRSL1c selection. In this signal region, Z + jets production, with the Z boson decaying to neutrinos, plus a nonprompt muon related to one of the jets, constitutes a non-negligible contribution. This contribution is estimated from simulation, together with a correction derived from a data sample of events with two or more muons, selected by the single-muon trigger. In this control sample, Z + jets events with Z boson decays to muon pairs are used. By using tighter muon selection criteria and restricting the mass of the dimuon system to be within 15 GeV of m(Z), a high-purity sample is obtained. The events are used to mimic $Z \to \nu\nu$ decays by removing the two daughter muons and adding their momenta to the E_T^{miss} vector. The correction is applied as the product of two factors: $R_{\mu\mu}$, the inclusive data-to-simulation ratio, and $R_{\mu\mu\mu/\mu\mu}$, the ratio of the probabilities to observe a third, soft muon. The first factor corrects the cross section in the $\mu\mu$ channel for a signal-like region. Its measured value is 0.80 ± 0.03. The double ratio $R_{\mu\mu\mu/\mu\mu}$ is determined in a looser selection to be 1.26 ± 0.27, yielding a total correction factor of 1.01 ± 0.22. The uncertainties quoted above are statistical. Systematic uncertainties due to the evolution with E_T^{miss} and H_T, or due to differences in the muon efficiency or acceptance between data and simulation, are negligible with respect to the statistical uncertainty.

The contribution from multijet events is estimated by inverting the requirements on muon isolation, the muon impact parameter, and the veto on leading jets in back-to-back configuration. Assuming small correlations among the three variables mentioned above, the yield of multijet events can be estimated from the yield obtained with the fully inverted selection combined with the product of three reduction factors (one for each variable). The estimated contributions to SRSL1 and SRSL2 are below 0.1 events and are therefore neglected.

A summary of the expected contributions of different background processes to the SRs is shown in Table 3 together with the yields of two benchmark signal points.

4.2. Background systematic uncertainties

In addition to the systematic uncertainties estimated in the previous subsections, the following systematic effects and associated uncertainties have been evaluated.

The full difference in the background estimates induced by the correction of the p_T spectrum of simulated $t\bar{t}$ and W + jets events is assigned as a systematic uncertainty. The impact of the reweighting applied to $t\bar{t}$ events is only significant for the signal region SRSL2, where the contribution of this background is the highest.

Changes in the polarization of the W boson can have an impact on the results since they change the balance between muon p_T and E_T^{miss}. To quantify this effect, the polarization fractions $f_{\lambda=+1}$, $f_{\lambda=-1}$, and $f_{\lambda=0}$, associated with helicity $+1$, -1, and 0 amplitudes have been modified following three different scenarios: a 10% variation of $f_{-1} - f_{+1}$ for both W^+ and W^-, a 5% variation of f_{-1}, f_{+1}, and a 10% variation of the longitudinal polarization fraction f_0 [51–53].

Table 3
Estimated background contributions for the signal regions of the single-muon analysis. The scale factors determined in the control regions are applied. For the signal samples, $m(\tilde{t})$ and $m(\tilde{\chi}_1^0)$ are shown in parentheses. All uncertainties are statistical.

Background	SRSL1a	SRSL1b	SRSL1c	SRSL2
W + jets	116.8 ± 8.8	73.2 ± 7.6	8.8 ± 2.1	16.0 ± 4.9
$t\bar{t}$	7.4 ± 1.3	4.1 ± 1.0	1.2 ± 0.5	13.8 ± 1.8
$Z \to \nu\nu$ + jets	1.1 ± 0.4	1.2 ± 0.4	1.5 ± 0.5	0.3 ± 0.2
$Z/\gamma^* \to \ell\ell$ + jets	4.4 ± 0.5	0.2 ± 0.1	0.2 ± 0.1	0.5 ± 0.2
VV	4.6 ± 0.7	1.8 ± 0.5	0.7 ± 0.3	0.5 ± 0.2
Single top quark	0.1 ± 0.1	0.6 ± 0.4	< 0.3	1.0 ± 0.7
Total SM	134.5 ± 8.9	81.3 ± 7.8	12.3 ± 2.3	32.1 ± 5.3
$\tilde{t}\tilde{t}$ signal (250, 230)	32.5 ± 2.8	6.2 ± 1.2	4.7 ± 1.0	7.1 ± 1.3
$\tilde{t}\tilde{t}$ signal (300, 250)	11.0 ± 1.0	4.2 ± 0.6	5.1 ± 0.7	10.7 ± 1.0

Table 4
Relative systematic uncertainties in the background predictions in the signal regions of the single-muon search. The labels refer to sources of systematic uncertainties discussed in Sections 3 and 4.2.

Systematic effect	Uncertainty (%)			
	SRSL1a	SRSL1b	SRSL1c	SRSL2
Pileup	0.5	0.8	3.0	0.5
W p_T reweighting	7.1	8.8	8.1	3.7
$t\bar{t}$ p_T reweighting	0.8	0.5	0.1	5.4
Jet energy scale	2.4	3.2	2.1	6.0
Jet energy resolution	1.1	4.4	7.3	3.4
b tagging	0.1	0.1	0.5	1.3
W polarization	2.9	2.8	3.9	0.8
Muon efficiency	3.5	3.5	3.5	3.5
W + jets validation	8.8	18.1	21.7	10.2
$t\bar{t}$ validation	1.0	0.9	1.7	8.4
Other backgrounds	3.8	2.4	9.8	3.6
Total uncertainty	13.1	21.5	27.0	17.1

The uncertainties based on the comparison of data and simulation in the validation regions described in the previous subsection are propagated to the final estimate. An uncertainty of 50% is assigned to the cross sections of all non-leading backgrounds, including $Z \to \nu\nu$, and propagated through the full estimation procedure. An overview of all systematic uncertainties related to the background prediction is presented in Table 4. The dominant uncertainties are related to the limited statistical precision of the validation procedure and to the uncertainties in the shape of the muon p_T spectrum in W + jets events.

5. Search in the dilepton channel

The analysis in the dilepton channel also starts from the common baseline selection described in Section 3. In this topology, less background is expected, and thus the selection requirements on E_T^{miss} and the p_T of the ISR jet candidate are set to be above 200 and 150 GeV, respectively, just above the trigger thresholds. To increase sensitivity, we select events in two signal regions defined by the p_T of the leading lepton: 5–15 and 15–25 GeV. The second lepton is required to have $p_T < 15$ GeV. We require exactly two identified leptons of opposite sign, with at least one of them a muon. Finally, events with an invariant mass of the dilepton pair $m(\ell\ell) < 5$ GeV are rejected to remove a region that is difficult to simulate and to avoid any potential J/ψ background. Because the relative fraction of reconstructed leptons not arising from the decay of a W or Z boson ("nonprompt" leptons) is higher compared to the single-lepton channel, the isolation and identification criteria on the leptons are stricter. On top of the muon identification used for the single-lepton topology, stricter requirements on the number of tracker hits, the quality of the track fit, and the match to signals in the muon detector are applied. This selection is similar to the soft muon identification used for b-quark physics in CMS [54]. For electrons, the definitions for the $H \to ZZ \to 4\ell$ [55] analysis are used together with a stronger rejection of photon conversions. For both flavours, the leptons are required to be isolated ($I_{abs} < 5$ GeV and $I_{rel} < 0.5$) and to have impact parameter values d_{xy} and d_z smaller than 0.01 cm. As in the region SRSL1 of the single-muon analysis, b-tagged jets are vetoed to suppress $t\bar{t}$ backgrounds. To remove potential multijet backgrounds, a selection on $E_T^{miss}/H_T > 2/3$ is applied.

After this selection, one of the main backgrounds is Z/γ^* production of τ pairs, with both τ leptons decaying leptonically. Under the assumption that the direction of the reconstructed lepton is parallel to the τ direction, which is true to good approximation, the invariant mass of the τ pair, $m_{\tau\tau}$, can be reconstructed by setting its transverse momentum equal to the hadronic recoil (the missing transverse momentum without the leptons). All events with $m_{\tau\tau} < 160$ GeV are rejected.

The definitions of the dilepton signal (SRDL) and control (CRDL) regions are summarized in Table 5.

5.1. Background prediction

Four different background categories are predicted from data: dileptonic $t\bar{t}$ events ($t\bar{t}(2\ell)$, $\ell : e\mu\tau$), which constitute the largest background; diboson production such as WW or WZ (the second-largest background); and Z/γ^* production of τ pairs with leptonic τ decays. Backgrounds with one nonprompt lepton, i.e. W + jets and semileptonic $t\bar{t}$ events ($t\bar{t}(1\ell)$), are the fourth category. Half of the background events contain at least one τ lepton that decays leptonically. The negligible (≈1%) contribution of rare processes ($t\bar{t}V$, $t\bar{t}H$, tW, and $W^{\pm}W^{\pm}$) is predicted by using simulation. For each of the four categories, a CR enriched in such processes is defined in data, from which we derive correction factors to correct yields from simulation.

In all CRs, the requirements on jets are the same as in the SR. Several CRs use events with higher lepton p_T compared to the SR. In these regions, the leading lepton has to be a muon, and events are selected by using the single-muon trigger described before. The relative lepton isolation has to be smaller than 0.12 and the muon identification criteria are tightened. Apart from the Z/γ^* control region, the E_T^{miss} requirement is lowered to 125 GeV and the E_T^{miss} selection of the signal region is instead applied to L_T, the sum of E_T^{miss} and the p_T of the leading lepton. The present selection is $L_T > 225$ GeV to take into account that for the default selection L_T is also up to 25 GeV higher than E_T^{miss}. In this way, the event yields in the CRs can be increased while maintaining kinematics similar to the SR even in the presence of a higher-p_T lepton.

To achieve a clean control sample of dileptonic $t\bar{t}$ events (CRDL($t\bar{t}(2\ell)$)), we require exactly one b-tagged jet. This jet must

Table 5
Definition of signal and control regions for the dilepton search. For the CRs, only changes with respect to the SR are shown. Dashes indicate that no selection is applied. For the lower limits on lepton p_T in the SR, the value used for electrons is shown in parentheses. The SR is subdivided into two bins according to the p_T of the leading lepton: 5–15 and 15–25 GeV.

Variable	SRDL	CRDL					
		$t\bar{t}(2\ell)$	NPR1	NPR2	VV	Z	$\tau\tau$
$Q(\ell_1)Q(\ell_2)$	-1		$+1$	$+1$			
$\ell_1\ \ell_2$	$\mu\mu$, μe, eμ	$\mu\mu$, μe		$\mu\mu$, μe	$\mu\mu$, μe	$\mu\mu$	
$p_T(\ell_1)$ (GeV)	5(7)–25	> 25		> 25	> 25	> 125	
$p_T(\ell_2)$ (GeV)	5(7)–15	> 15			> 15	> 10	
$\lvert\eta\rvert(\ell)$	< 1.5					< 2.1	
d_{xy}, $d_z(\ell)$ (cm)	< 0.01					< 0.02, < 0.5	
p_T (ISR jet) (GeV)	> 150						
p_T (jet3) (GeV)	< 60						
Number of b jets	0	1			0 (loose id.)		
Number of jets	≥ 1				1 or 2		
$\lvert\Delta\phi(\ell_1, \text{ISR jet})\rvert$ (rad)	–				> 1		
E_T^{miss} (GeV)	> 200	> 125		> 125	> 125	–	
E_T^{miss}/H_T	$> 2/3$	–		–	–	–	
L_T (GeV)	–	> 225		> 225	> 225	–	
L_T/H_T	–	$> 2/3$		$> 2/3$	$> 2/3$		
$p_T(\mu\mu)$ (GeV)	–					> 200	
$p_T(\mu\mu)/H_T$	–					$> 2/3$	
$m(\ell\ell)$ (GeV)	> 5				> 50	> 10	
$m(\tau\tau)$ (GeV)	> 160					–	< 160

not be the leading jet to ensure a distribution in p_T of the $t\bar{t}$ system similar to that in the SR. We require one muon with $p_T > 25$ GeV and a subleading lepton with $p_T > 15$ GeV. Backgrounds other than $t\bar{t}(2\ell)$ are subtracted from data before calculating the ratio between data and the prediction from simulation for $t\bar{t}(2\ell)$ in the CR. This ratio is used to rescale the simulated $t\bar{t}(2\ell)$ yields in the SR.

For the CR enriched in nonprompt leptons (CRDL(NPR)), we use the union of two samples. The first sample (CRDL(NPR1)) corresponds to the SR with the exception that the leptons are required to have the same charge. It was checked that in the selected kinematic region, the origins for NPR leptons, mainly heavy quarks, occur at a similar fraction as in the SR. In addition, the kinematics of these nonprompt leptons is very similar in signal and control regions. For the second sample (CRDL(NPR2)), same-sign events with a leading lepton p_T above 25 GeV are used, and the CR selection of $E_T^{miss} > 125$ GeV, $L_T > 125$ GeV, and $L_T/H_T > 2/3$ is applied. Under these conditions the origins and kinematics of the nonprompt leptons are similar between signal and control regions, since the NPR contribution in the signal region is mostly related to the subleading lepton. Again the data yield in the combined CR is corrected for other backgrounds, such as diboson events, by using simulation. The ratio of the corrected yield to the simulated NPR yield in the CR is used to rescale the simulated NPR yield in the SR.

For the prediction of Z/γ^* events, two separate CRs are defined. The first one is used to correct for any effects on $m_{\tau\tau}$ (CRDL(Z)). For this purpose, a clean sample of Z/γ^* events with decays to a pair of muons is used. The invariant mass of the muon pair has to be higher than 10 GeV and the E_T^{miss} selection is applied to the p_T of the muon pair. Three bins are defined as a function of this momentum: 200–300, 300–400, and > 400 GeV. We use the reconstructed muon pair p_T to measure the resolution of the hadronic recoil along and perpendicular to the direction given by the muon pair both in data and simulation. The resulting scaling factors of the recoil resolution are applied to the simulation to recompute the efficiency of the $m_{\tau\tau}$ selection in the SR. A second control region (CRDL($\tau\tau$)) is used to measure in data the probability of $Z/\gamma^* \to \tau\tau$ events leading to two soft leptons and very high E_T^{miss}. To do so, we use the SRDL selection with the requirement on $m_{\tau\tau}$ inverted to < 160 GeV. After subtracting other backgrounds in this region by using simulation, the observed yield is multiplied by the corrected $m_{\tau\tau}$ efficiency to predict the number of Z/γ^* events in the SR.

For the diboson control region (CRDL(VV)) one muon with $p_T > 25$ GeV is required. The p_T of the second lepton has to be > 15 GeV. To further enhance the diboson fraction and reduce the otherwise dominant $t\bar{t}$ background, at most two jets are allowed, events with a jet passing a looser working point of the b tagging algorithm are rejected, and the azimuthal angle between the leading lepton and the leading jet has to be > 1 rad. Finally, we require $m_{\ell\ell}$ to be above 50 GeV. Contributions of $t\bar{t}(2\ell)$, NPR, and Z/γ^* to CRDL(VV) are estimated with methods similar to those used for the SR. Backgrounds due to rare processes are subtracted by using the simulation. After this correction, the ratio of the number of data to simulated diboson events is built and used to rescale the simulated VV yield in the SR.

The background contribution from multijet events is negligible in our final selection. Apart from the fact that we require high E_T^{miss} and two leptons, we also select $E_T^{miss}/H_T > 2/3$ to reject any residual multijet events. To evaluate the efficacy of this selection, a test was performed by inverting this requirement to have a region that should have significant multijet background if there were any. For this region, data yields were compared with the simulation results of all considered background categories (which do not include multijet events) and were found to be in agreement. Further tests were performed by using the electron–electron channel and by relaxing the upper limits on d_{xy} and d_z to 0.05 cm, which showed no indication for a contamination by multijet events. These tests confirmed that, as expected, we can assume that multijet background is negligible in our final selection that employs much tighter requirements against multijet events.

The event yields for data and simulation in the different CRs that are the basis for the scale factors applied in the SRs are shown in Table 6. The predicted event yields per background for each search bin are presented in Table 7. The impact of a potential signal contamination is found to be only relevant for control regions CRDL(NPR) and CRDL($\tau\tau$), with an effect of a few percent on the total background prediction in the signal regions, and is taken into account in the statistical analysis of the results.

To test the prediction methods, we define several validation regions that are enriched in specific backgrounds but expected to be free of signal. The first region is equivalent to the signal region, except for an inversion of the veto on b-tagged jets. This region

Table 6
Contributions to the control regions of the dilepton analysis as expected from simulation before application of scale factors, together with the observed event counts. All uncertainties are statistical.

Background	CRDL($t\bar{t}(2\ell)$)	CRDL(NPR)	CRDL(VV)	CRDL($\tau\tau$)
$t\bar{t}(2\ell)$	119.1 ± 2.4	0.27 ± 0.11	30.3 ± 1.2	0.15 ± 0.08
$t\bar{t}(1\ell)$	1.09 ± 0.29	4.7 ± 0.6	0.30 ± 0.14	0.11 ± 0.11
W + jets	< 0.4	3.4 ± 1.3	< 0.4	0.7 ± 0.7
Z/γ^* + jets	0.4 ± 0.4	< 0.30	4.9 ± 1.3	2.8 ± 0.9
VV	2.4 ± 0.6	0.62 ± 0.11	45.9 ± 1.8	0.13 ± 0.09
Rare backgrounds	14.9 ± 2.7	1.0 ± 0.5	6.4 ± 1.7	< 0.21
Total SM background	138.0 ± 3.7	10.0 ± 1.5	87.8 ± 3.0	3.9 ± 1.1
Data	119	11	8	5

Table 7
Estimated background contributions for the two signal regions of the dilepton search. The scale factors determined in the control regions are applied. For the signal samples, $m(\tilde{t})$ and $m(\tilde{\chi}_1^0)$ are shown in parentheses. All uncertainties are statistical.

Background	$p_T(\ell_1)$: 5–15 GeV	$p_T(\ell_1)$: 15–25 GeV	Inclusive
$t\bar{t}(2\ell)$	0.75 ± 0.19	2.08 ± 0.37	2.8 ± 0.4
$t\bar{t}(1\ell)$, W + jets	0.60 ± 0.33	1.3 ± 0.7	1.9 ± 0.8
Z/γ^* + jets	< 0.30	0.5 ± 0.5	0.5 ± 0.5
VV	0.74 ± 0.27	1.6 ± 0.5	2.4 ± 0.5
Rare backgrounds	0.03 ± 0.01	0.08 ± 0.04	0.11 ± 0.04
Total SM background	2.1 ± 0.5	5.6 ± 1.0	7.7 ± 1.1
$\tilde{t}\tilde{t}$ signal (225, 145)	4.2 ± 1.2	6.3 ± 1.6	10.4 ± 2.0
$\tilde{t}\tilde{t}$ signal (300, 250)	4.0 ± 0.6	3.8 ± 0.6	7.8 ± 0.8

is used to test the prediction of low-p_T leptons in $t\bar{t}(2\ell)$ events. The next validation region is identical to CRDL($t\bar{t}(2\ell)$), except that the p_T of the subleading lepton is required to be below 15 GeV. This region provides a further test of the prediction of the soft-lepton rate. Another validation region is the same as CRDL(VV), apart from the fact that all selections used to enrich the region in diboson events are inverted. In addition, a validation region that has a composition in backgrounds similar to the signal region is defined. For this, one muon with p_T above 25 GeV is required, while the second lepton must be soft ($p_T < 15$ GeV). All validation regions show reasonable agreement between prediction and observation.

5.2. Background systematic uncertainties

In addition to the common uncertainties from object reconstruction and simulation as described in Sections 2 and 3, the following systematic uncertainties that are specific to the individual background predictions are considered.

In estimating the $t\bar{t}(2\ell)$ background, the polarization of the W boson resulting from the top quark decay is varied. In addition, the spin correlation between the two top quarks is changed by 20%, since this might affect how often both leptons are soft [56]. As in the single-lepton channel, the difference due to the reweighting of the top quark p_T spectrum in $t\bar{t}$ simulation is taken as a further uncertainty. However, its effect is small due to the background prediction method used.

For a conservative assessment of the uncertainty related to the estimate of NPR backgrounds, the fractions of leptons from b and c hadrons are varied by 50% and 100%, respectively. The relative fraction of $t\bar{t}$ to W + jets events is altered by rescaling both contributions by ±50%. The largest of these variations is used as the uncertainty. Furthermore, the p_T and $|\eta|$ distributions in the CR are varied to reflect potential residual differences in the kinematics between signal and control regions. Moreover, the polarization of the W boson is varied to estimate the uncertainty due to polarization modelling.

Table 8
Relative systematic uncertainties in the background predictions in the signal regions of the dilepton search.

Systematic effect	Uncertainty (%)	
	$p_T(\ell_1)$: 5–15 GeV	$p_T(\ell_1)$: 15–25 GeV
Statistical uncertainty	21.9	18.3
Jet energy scale	1.0	2.8
b tagging	1.5	1.4
Electron efficiency	1.3	1.1
Muon efficiency	6.0	4.5
$t\bar{t}$ background	5.1	5.4
NPR background	10.1	5.6
Z/γ^* background	< 0.1	2.3
VV background	8.0	2.6
Rare backgrounds	3.7	3.3
Total uncertainty	26.9	21.1

The cross sections for WW [57,58] and also WZ and ZZ [59] production have been measured at the LHC, and both the total and differential cross sections show reasonable agreement between data and simulation. To estimate the uncertainties related to VV production, the polarization of the vector bosons is altered by 10%, as well as the fraction of the diboson pair momentum that a single boson carries. In addition, the cross section corresponding to events with low $m(\gamma^*)$ between 5 and 12 GeV is varied by 100% to account for any potential shape mismodelling of the dilepton mass.

In the estimation of the Z/γ^* background, the effect of the recoil resolution correction is used to derive an uncertainty due to a potential mismodelling of the resolution. The cross section of rare processes is varied by ±50% throughout the analysis (also in the CRs), and the effect is propagated to the event yields in the SR.

A summary of all uncertainties can be found in Table 8. The dominating uncertainty stems from the limited number of simulated events with nonprompt leptons in the SRs.

Table 9
Summary of observed and expected background yields in the signal regions of the single-lepton and dilepton searches. The uncertainties in the background yields include statistical and systematic contributions. Transverse momenta are shown in units of GeV.

Single muon						Dilepton		
$p_T(\mu)$		SRSL1a	SRSL1b	SRSL1c	SRSL2	$p_T(\ell_1)$		SRDL
5–12	exp.	41.1 ± 6.3	29.7 ± 7.2	4.3 ± 1.5	11.3 ± 2.9	5–15	exp.	2.1 ± 0.6
	obs.	42	17	3	16		obs.	2
12–20	exp.	44.2 ± 6.8	25.1 ± 6.2	3.1 ± 1.2	8.5 ± 2.4	15–25	exp.	5.6 ± 1.2
	obs.	39	14	4	16		obs.	4
20–30	exp.	49.2 ± 7.5	26.5 ± 6.5	5.0 ± 1.8	12.2 ± 3.0			
	obs.	40	28	5	9			
All	exp.	134.5 ± 19.8	81.3 ± 19.1	12.3 ± 4.0	32.1 ± 7.7	All	exp.	7.7 ± 1.4
	obs.	121	59	12	41		obs.	6

6. Results and interpretation

The observations and background predictions for the signal regions of the single-lepton and dilepton searches are summarized in Table 9. Observed and predicted yields are in good agreement and give no indication of the presence of signal.

The modified-frequentist CL_S method [60–62] with a one-sided profile likelihood ratio test statistic is used to define 95% confidence level (CL) upper limits on the production cross section as a function of the sparticle masses. Statistical uncertainties related to the observed number of events in CRs are modelled as Poisson distributions. All other uncertainties are assumed to be multiplicative and are modelled with log-normal distributions. The impact of a potential signal contamination in the control regions is taken into account in the calculation of the limits for each signal point.

Systematic uncertainties in the signal yields related to the determination of the integrated luminosity [63] (2.6%), pileup (≈ 2%), energy scales [35,36] (up to 7%), object identification efficiencies [40,41] (up to 10%), and uncertainties in the parton distribution functions [64–68] (up to 6%) and the modelling of ISR [48] (≈ 20%) have been evaluated. Correlations between the systematic uncertainties in different signal regions are taken into account, where applicable. All systematic uncertainties are treated as nuisance parameters in the calculation of the limits, with the exception of the theoretical uncertainty on the inclusive SUSY production cross section. The latter is shown in the form of an up- and downward variation of the observed mass limits.

The limits obtained for top squark pair production in the single-muon and the dilepton searches are shown in Fig. 3 top and bottom, respectively, under the assumption of a 100% branching fraction of the four-body decay. By using the $\tilde{t}$ pair production cross section calculated at next-to-leading order (NLO) + next-to-leading logarithm (NLL) precision [69–73], the cross section limits can be converted into excluded regions in the $\tilde{t}$–$\tilde{\chi}_1^0$ mass plane. Uncertainties in these cross sections are determined as detailed in Ref. [74]. At $\Delta m = 25$ GeV, the dilepton search excludes $\tilde{t}$ masses below 316 GeV. Here and in the following all quoted values for mass limits conservatively refer to the -1σ variation of the predicted cross section. The single-muon search shows a smaller reach in $m(\tilde{t})$ (≈ 250 GeV) but has a higher sensitivity at the lowest considered mass splitting of 10 GeV, where values up to ≈ 210 GeV are excluded. In the intermediate Δm region (≈ 20–70 GeV), these results considerably extend existing limits [19–21]. They are complementary to the results of searches in the monojet topology [18,19,21].

In the case of chargino–neutralino pair production, the results of the dilepton analysis are used. For the model involving decay chains with sleptons, the slepton masses are set to $(m(\tilde{\chi}_1^0) + m(\tilde{\chi}_1^+))/2$. Instead of using branching fractions derived from complete SUSY models, two extreme decay scenarios are studied in order to illustrate the dependence on the final state. In the "flavour-democratic" scenario, both the neutralino and the chargino would decay via the supersymmetric partners of the left-handed leptons ($\tilde{\ell}_L$) and of the neutrinos ($\tilde{\nu}$) with equal branching fractions to all

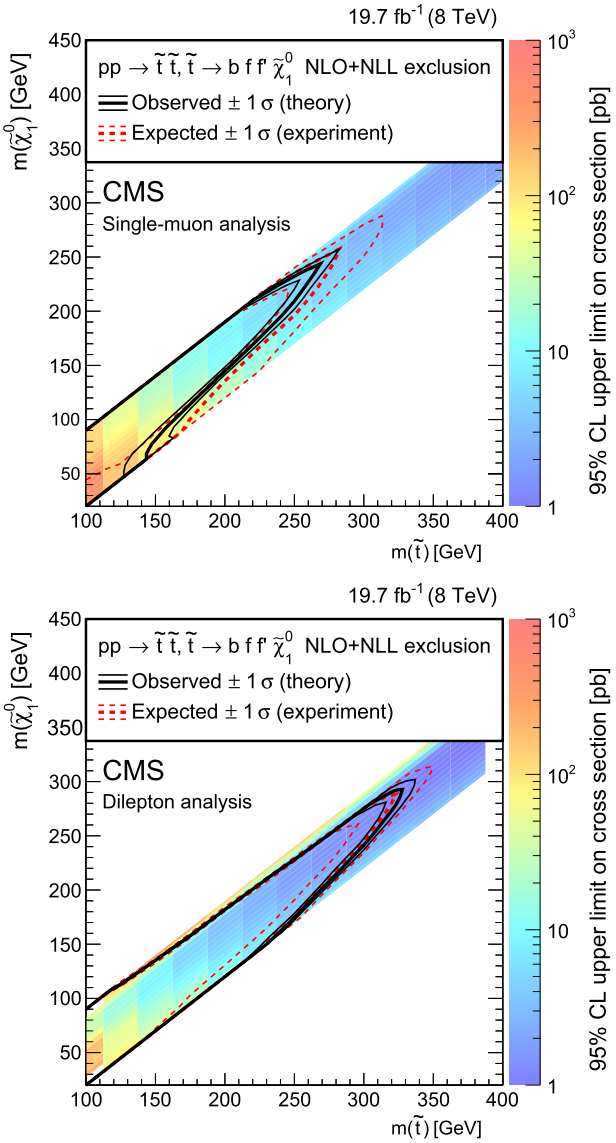

Fig. 3. Cross section and mass limits at 95% CL in the $m(\tilde{\chi}_1^0)$ and $m(\tilde{t})$ mass plane for the (top) single-muon and (bottom) dilepton searches. The colour shading corresponds to the observed limit on the cross section. The solid (dashed) lines show the observed (expected) mass limits, with the thick lines representing the central value and the thin lines the variations due to the theoretical (experimental) uncertainties.

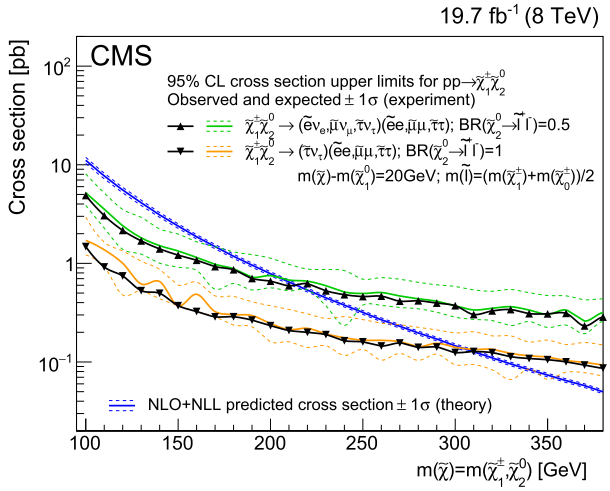

Fig. 4. Cross section limits at 95% CL obtained from the search in the dilepton channel as a function of the common $\widetilde{\chi}_1^{\pm}/\widetilde{\chi}_1^0$ mass. The black lines with symbols correspond to the observed limit, while the solid and dashed coloured lines represent the expected limit and the $\pm 1\sigma$ bands corresponding to the experimental uncertainties, respectively. The flavour-democratic (τ-enriched) cases of the model are indicated by green (orange) lines and upward- (downward-) pointing triangular symbols. The solid and dashed blue lines without symbols correspond to the predicted cross section for chargino–neutralino production and its uncertainties. (For interpretation of the references to colour in this figure legend, the reader is referred to the web version of this article.)

lepton flavours. In this scenario, the fraction of events with at least two charged leptons is reduced by 50% due to the $\widetilde{\chi}_2^0 \to \nu\nu\widetilde{\chi}_1^0$ decay channel. In the "τ-enriched" scenario, the decays would proceed via the supersymmetric partners of the right-handed leptons. In this case, the decay $\widetilde{\chi}_2^0 \to \nu\nu\widetilde{\chi}_1^0$ is not present, and we assume equal branching fractions of the $\widetilde{\chi}_2^0$ into the three charged lepton flavours and exclusive decays of the chargino to τ leptons. In Fig. 4, the 95% CL cross section limits are presented for a mass splitting of $\Delta m \equiv m(\widetilde{\chi}) - m(\widetilde{\chi}_1^0) = 20$ GeV. Comparing with the predicted cross section, calculated at NLO + NLL precision with the Resummino [75–77] program, 95% CL limits on $m(\widetilde{\chi})$ of 212 and 307 GeV are obtained for the flavour-democratic and τ-enriched scenarios, respectively. In these compressed scenarios, the new limits slightly improve current results [25,29] in the flavour-democratic scenario and exceed them by ≈ 200 GeV for the τ-enriched scenario. As for the latter case, the dominant decays lead to final states with opposite-sign leptons.

7. Summary

A search for supersymmetry with compressed mass spectra is performed in events with soft leptons, moderate to high values of $E_{\mathrm{T}}^{\mathrm{miss}}$, and one or two hard jets, compatible with the emission of initial-state radiation. The data sample corresponds to 19.7 fb^{-1} of proton–proton collisions recorded by the CMS experiment at $\sqrt{s} =$ 8 TeV. Two event categories are considered: events with a single, soft muon and events in which a second, soft electron or muon is present.

The first target of this search is the pair production of top squarks with a mass splitting of at most 80 GeV with respect to the LSP. At low mass splitting, lepton momenta are low, and the b jets do not enter the acceptance. At higher values of Δm, the average lepton momentum increases and soft b jets can be reconstructed. Therefore, signal regions are further divided according to the p_{T} of the leading lepton and the presence or absence of a soft b-tagged jet. In the single-lepton search the transverse mass of the lepton-$E_{\mathrm{T}}^{\mathrm{miss}}$ system is used as an additional discriminant.

The main backgrounds to this search are W + jets and $\mathrm{t\bar{t}}$ production. Contributions to the signal regions from these and several nonleading background sources are estimated by using data in control regions to normalize the simulated yields. These estimates are tested with data in validation regions.

The observations in the signal regions are compatible with the SM background predictions. In the absence of any indication of signal, cross section limits are set at 95% CL in the $\widetilde{\mathrm{t}}$–$\widetilde{\chi}_1^0$ mass plane. These results are used to extract mass limits based on a reference cross section for top squark pair production and assuming a 100% branching fraction for the four-body decay $\widetilde{\mathrm{t}} \to \mathrm{bff}'\widetilde{\chi}_1^0$. The most stringent limit on the mass of the top squark is obtained in the dilepton channel: $m(\widetilde{\mathrm{t}}) > 316$ GeV at 95% CL for a mass splitting of 25 GeV. These results extend existing limits in the four-body decay channel of the top squark [19–21] and complement the analyses performed in the $\widetilde{\mathrm{t}} \to \mathrm{c}\widetilde{\chi}_1^0$ channel [18,21].

The results obtained in the dilepton channel are also used to set limits on models of chargino–neutralino production in a compressed spectrum with a mass difference between $\widetilde{\chi}_2^0/\widetilde{\chi}_1^+$ and $\widetilde{\chi}_1^0$ of 20 GeV. Based on the 95% CL upper limit on the cross section in the case of flavour-democratic leptonic decays of these particles, a lower limit on the common $\widetilde{\chi}_1^+/\widetilde{\chi}_2^0$ mass is set at 212 GeV. If chargino decays proceed exclusively via the τ channel, and in the absence of the $\widetilde{\chi}_2^0 \to \widetilde{\nu}\nu$ decay mode, this limit increases to 307 GeV, well above existing limits [25,29].

Acknowledgements

We congratulate our colleagues in the CERN accelerator departments for the excellent performance of the LHC and thank the technical and administrative staffs at CERN and at other CMS institutes for their contributions to the success of the CMS effort. In addition, we gratefully acknowledge the computing centres and personnel of the Worldwide LHC Computing Grid for delivering so effectively the computing infrastructure essential to our analyses. Finally, we acknowledge the enduring support for the construction and operation of the LHC and the CMS detector provided by the following funding agencies: BMWFW and FWF (Austria); FNRS and FWO (Belgium); CNPq, CAPES, FAPERJ, and FAPESP (Brazil); MES (Bulgaria); CERN; CAS, MOST, and NSFC (China); COLCIENCIAS (Colombia); MSES and CSF (Croatia); RPF (Cyprus); MoER, ERC IUT and ERDF (Estonia); Academy of Finland, MEC, and HIP (Finland); CEA and CNRS/IN2P3 (France); BMBF, DFG, and HGF (Germany); GSRT (Greece); OTKA and NIH (Hungary); DAE and DST (India); IPM (Iran); SFI (Ireland); INFN (Italy); MSIP and NRF (Republic of Korea); LAS (Lithuania); MOE and UM (Malaysia); CINVESTAV, CONACYT, SEP, and UASLP-FAI (Mexico); MBIE (New Zealand); PAEC (Pakistan); MSHE and NSC (Poland); FCT (Portugal); JINR (Dubna); MON, RosAtom, RAS, and RFBR (Russia); MESTD (Serbia); SEIDI and CPAN (Spain); Swiss Funding Agencies (Switzerland); MST (Taipei); ThEPCenter, IPST, STAR and NSTDA (Thailand); TUBITAK and TAEK (Turkey); NASU and SFFR (Ukraine); STFC (United Kingdom); and DOE and NSF (USA).

Individuals have received support from the Marie-Curie programme and the European Research Council and EPLANET (European Union); the Leventis Foundation; the Alfred P. Sloan Foundation; the Alexander von Humboldt Foundation; the Belgian Federal Science Policy Office; the Fonds pour la Formation à la Recherche dans l'Industrie et dans l'Agriculture (FRIA-Belgium); the Agentschap voor Innovatie door Wetenschap en Technologie (IWT-Belgium); the Ministry of Education, Youth and Sports (MEYS) of the Czech Republic; the Council of Science and Industrial Research, India; the HOMING PLUS programme of the Foundation for Polish Science, cofinanced from European Union, Regional Development Fund; the OPUS programme of the National Science Cen-

ter (Poland); the Compagnia di San Paolo (Torino); MIUR project 20108T4XTM (Italy); the Thalis and Aristeia programmes cofinanced by EU-ESF and the Greek NSRF; the National Priorities Research Program by Qatar National Research Fund; the Rachadapisek Sompot Fund for Postdoctoral Fellowship, Chulalongkorn University (Thailand); the Chulalongkorn Academic into Its 2nd Century Project Advancement Project (Thailand); and the Welch Foundation, contract C-1845.

References

[1] J. Wess, B. Zumino, Supergauge transformations in four dimensions, Nucl. Phys. B 70 (1974) 39, http://dx.doi.org/10.1016/0550-3213(74)90355-1.
[2] H.P. Nilles, Supersymmetry, supergravity and particle physics, Phys. Rep. 110 (1984) 1, http://dx.doi.org/10.1016/0370-1573(84)90008-5.
[3] H.E. Haber, G.L. Kane, The search for supersymmetry: probing physics beyond the standard model, Phys. Rep. 117 (1985) 75, http://dx.doi.org/10.1016/0370-1573(85)90051-1.
[4] R. Barbieri, S. Ferrara, C.A. Savoy, Gauge models with spontaneously broken local supersymmetry, Phys. Lett. B 119 (1982) 343, http://dx.doi.org/10.1016/0370-2693(82)90685-2.
[5] S. Dawson, E. Eichten, C. Quigg, Search for supersymmetric particles in hadron–hadron collisions, Phys. Rev. D 31 (1985) 1581, http://dx.doi.org/10.1103/PhysRevD.31.1581.
[6] E. Witten, Dynamical breaking of supersymmetry, Nucl. Phys. B 188 (1981) 513, http://dx.doi.org/10.1016/0550-3213(81)90006-7.
[7] S. Dimopoulos, H. Georgi, Softly broken supersymmetry and SU(5), Nucl. Phys. B 193 (1981) 150, http://dx.doi.org/10.1016/0550-3213(81)90522-8.
[8] G.R. Farrar, P. Fayet, Phenomenology of the production, decay, and detection of new hadronic states associated with supersymmetry, Phys. Lett. B 76 (1978) 575, http://dx.doi.org/10.1016/0370-2693(78)90858-4.
[9] R. Barbieri, G. Giudice, Upper bounds on supersymmetric particle masses, Nucl. Phys. B 306 (1988) 63, http://dx.doi.org/10.1016/0550-3213(88)90171-X.
[10] B. de Carlos, J. Casas, One-loop analysis of the electroweak breaking in supersymmetric models and the fine-tuning problem, Phys. Lett. B 309 (1993) 320, http://dx.doi.org/10.1016/0370-2693(93)90940-J, arXiv:hep-ph/9303291.
[11] M. Dine, W. Fischler, M. Srednicki, Supersymmetric technicolor, Nucl. Phys. B 189 (1981) 575, http://dx.doi.org/10.1016/0550-3213(81)90582-4.
[12] S. Dimopoulos, S. Raby, Supercolor, Nucl. Phys. B 192 (1981) 353, http://dx.doi.org/10.1016/0550-3213(81)90430-2.
[13] N. Sakai, Naturalness in supersymmetric GUTS, Z. Phys. C 11 (1981) 153, http://dx.doi.org/10.1007/BF01573998.
[14] R.K. Kaul, P. Majumdar, Cancellation of quadratically divergent mass corrections in globally supersymmetric spontaneously broken gauge theories, Nucl. Phys. B 199 (1982) 36, http://dx.doi.org/10.1016/0550-3213(82)90565-X.
[15] C. Balázs, M. Carena, C.E.M. Wagner, Dark matter, light stops and electroweak baryogenesis, Phys. Rev. D 70 (2004) 015007, http://dx.doi.org/10.1103/PhysRevD.70.015007, arXiv:hep-ph/0403224.
[16] A. Delgado, G.F. Giudice, G. Isidori, M. Pierini, A. Strumia, The light stop window, Eur. Phys. J. C 73 (2013) 2370, http://dx.doi.org/10.1140/epjc/s10052-013-2370-5, arXiv:1212.6847.
[17] R. Gröber, M.M. Mühlleitner, E. Popenda, A. Wlotzka, Light stop decays: implications for LHC searches, Eur. Phys. J. C 75 (2015) 420, http://dx.doi.org/10.1140/epjc/s10052-015-3626-z, arXiv:1408.4662.
[18] CMS Collaboration, Searches for third-generation squark production in fully hadronic final states in proton–proton collisions at $\sqrt{s} = 8$ TeV, J. High Energy Phys. 06 (2015) 116, http://dx.doi.org/10.1007/JHEP06(2015)116, arXiv:1503.08037.
[19] ATLAS Collaboration, Search for top squark pair production in final states with one isolated lepton, jets, and missing transverse momentum in $\sqrt{s} = 8$ TeV pp collisions with the ATLAS detector, J. High Energy Phys. 11 (2014) 118, http://dx.doi.org/10.1007/JHEP11(2014)118, arXiv:1407.0583.
[20] ATLAS Collaboration, Search for pair-produced third-generation squarks decaying via charm quarks or in compressed supersymmetric scenarios in pp collisions at $\sqrt{s} = 8$ TeV with the ATLAS detector, Phys. Rev. D 90 (2014) 052008, http://dx.doi.org/10.1103/PhysRevD.90.052008, arXiv:1407.0608.
[21] ATLAS Collaboration, ATLAS Run 1 searches for direct pair production of third-generation squarks at the Large Hadron Collider, Eur. Phys. J. C 75 (2015) 510, http://dx.doi.org/10.1140/epjc/s10052-015-3726-9, arXiv:1506.08616.
[22] G.F. Giudice, T. Han, K. Wang, L.-T. Wang, Nearly degenerate gauginos and dark matter at the LHC, Phys. Rev. C 81 (2010) 115011, http://dx.doi.org/10.1103/PhysRevD.81.115011, arXiv:1004.4902.
[23] P. Schwaller, J. Zurita, Compressed electroweakino spectra at the LHC, J. High Energy Phys. 03 (2014) 060, http://dx.doi.org/10.1007/JHEP03(2014)060, arXiv:1312.7350.
[24] Z. Han, G.D. Kribs, A. Martin, A. Menon, Hunting quasidegenerate Higgsinos, Phys. Rev. D 89 (2014) 075007, http://dx.doi.org/10.1103/PhysRevD.89.075007, arXiv:1401.1235.
[25] CMS Collaboration, Searches for electroweak production of charginos, neutralinos, and sleptons decaying to leptons and W, Z, and Higgs bosons in pp collisions at 8 TeV, Eur. Phys. J. C 74 (2014) 3036, http://dx.doi.org/10.1140/epjc/s10052-014-3036-7, arXiv:1405.7570.
[26] ATLAS Collaboration, Search for direct production of charginos and neutralinos in events with three leptons and missing transverse momentum in $\sqrt{s} = 8$ TeV pp collisions with the ATLAS detector, J. High Energy Phys. 04 (2014) 169, http://dx.doi.org/10.1007/JHEP04(2014)169, arXiv:1402.7029.
[27] ATLAS Collaboration, Search for the direct production of charginos, neutralinos and staus in final states with at least two hadronically decaying taus and missing transverse momentum in pp collisions at $\sqrt{s} = 8$ TeV with the ATLAS detector, J. High Energy Phys. 10 (2014) 96, http://dx.doi.org/10.1007/JHEP10(2014)096, arXiv:1407.0350.
[28] CMS Collaboration, Search for supersymmetry in the vector-boson fusion topology in proton–proton collisions at $\sqrt{s} = 8$ TeV, J. High Energy Phys. 11 (2015) 189, http://dx.doi.org/10.1007/JHEP11(2015)189, arXiv:1508.07628, 2015.
[29] ATLAS Collaboration, Search for the electroweak production of supersymmetric particles in $\sqrt{s} = 8$ TeV pp collisions with the ATLAS detector, Phys. Rev. D 93 (2016) 052002, http://dx.doi.org/10.1103/PhysRevD.93.052002, arXiv:1509.07152.
[30] CMS Collaboration, The CMS experiment at the CERN LHC, J. Instrum. 3 (2008) S08004, http://dx.doi.org/10.1088/1748-0221/3/08/S08004.
[31] CMS Collaboration, Particle-flow event reconstruction in CMS and performance for Jets, Taus, and E_T^{miss}, CMS Physics Analysis Summary CMS-PAS-PFT-09-001, 2009, http://cdsweb.cern.ch/record/1194487.
[32] CMS Collaboration, Commissioning of the particle-flow event reconstruction with the first LHC collisions recorded in the CMS detector, CMS Physics Analysis Summary CMS-PAS-PFT-10-001, 2010, http://cdsweb.cern.ch/record/1247373.
[33] M. Cacciari, G.P. Salam, G. Soyez, The anti-k_t jet clustering algorithm, J. High Energy Phys. 04 (2008) 063, http://dx.doi.org/10.1088/1126-6708/2008/04/063, arXiv:0802.1189.
[34] CMS Collaboration, Jet performance in pp collisions at 7 TeV, CMS Physics Analysis Summary CMS-PAS-JME-10-003, 2010, http://cdsweb.cern.ch/record/1279362.
[35] CMS Collaboration, Jet energy scale and resolution in the 8 TeV pp data, CMS Physics Analysis Summary CMS-PAS-JME-13-004, 2015, http://cdsweb.cern.ch/record/.
[36] CMS Collaboration, Performance of the CMS missing transverse momentum reconstruction in pp data at $\sqrt{s} = 8$ TeV, J. Instrum. 10 (2015) P02006, http://dx.doi.org/10.1088/1748-0221/10/02/P02006, arXiv:1411.0511.
[37] CMS Collaboration, Identification of b-quark jets with the CMS experiment, J. Instrum. 8 (2013) P04013, http://dx.doi.org/10.1088/1748-0221/8/04/P04013, arXiv:1211.4462.
[38] CMS Collaboration, Performance of b tagging at $\sqrt{s} = 8$ TeV in multijet, $t\bar{t}$ and boosted topology events, CMS Physics Analysis Summary CMS-PAS-BTV-13-001, 2013, http://cds.cern.ch/record/1581306.
[39] CMS Collaboration, Performance of τ-lepton reconstruction and identification in CMS, J. Instrum. 7 (2012) P01001, http://dx.doi.org/10.1088/1748-0221/7/01/P01001, arXiv:1109.6034.
[40] CMS Collaboration, Performance of electron reconstruction and selection with the CMS detector in proton–proton collisions at $\sqrt{s} = 8$ TeV, J. Instrum. 10 (2015) P06005, http://dx.doi.org/10.1088/1748-0221/10/06/P06005, arXiv:1502.02701.
[41] CMS Collaboration, Performance of CMS muon reconstruction in pp collision events at $\sqrt{s} = 7$ TeV, J. Instrum. 7 (2012) P10002, http://dx.doi.org/10.1088/1748-0221/7/10/P10002, arXiv:1206.4071.
[42] S. Frixione, P. Nason, C. Oleari, Matching NLO QCD computations with parton shower simulations: the POWHEG method, J. High Energy Phys. 11 (2007) 070, http://dx.doi.org/10.1088/1126-6708/2007/11/070, arXiv:0709.2092.
[43] T. Sjöstrand, S. Mrenna, P. Skands, PYTHIA 6.4 physics and manual, J. High Energy Phys. 05 (2006) 026, http://dx.doi.org/10.1088/1126-6708/2006/05/026, arXiv:hep-ph/0603175.
[44] J. Alwall, M. Herquet, F. Maltoni, O. Mattelaer, T. Stelzer, MadGraph 5: going beyond, J. High Energy Phys. 06 (2011) 128, http://dx.doi.org/10.1007/JHEP06(2011)128, arXiv:1106.0522.
[45] CMS Collaboration, Measurement of the underlying event activity at the LHC with $\sqrt{s} = 7$ TeV and comparison with $\sqrt{s} = 0.9$ TeV, J. High Energy Phys. 09 (2011) 109, http://dx.doi.org/10.1007/JHEP09(2011)109, arXiv:1107.0330.
[46] S. Agostinelli, et al., GEANT4 Collaboration, GEANT4 – a simulation toolkit, Nucl. Instrum. Methods Phys. Res., Sect. A, Accel. Spectrom. Detect. Assoc. Equip. 506 (2003) 250, http://dx.doi.org/10.1016/S0168-9002(03)01368-8.
[47] CMS Collaboration, The fast simulation of the CMS detector at LHC, J. Phys. Conf. Ser. 331 (2011) 032049, http://dx.doi.org/10.1088/1742-6596/331/3/032049.
[48] CMS Collaboration, Search for top-squark pair production in the single-lepton final state in pp collisions at $\sqrt{s} = 8$ TeV, Eur. Phys. J. C 73 (2013) 2677, http://dx.doi.org/10.1140/epjc/s10052-013-2677-2, arXiv:1308.1586.

[49] G. Arnison, et al., UA1 Collaboration, Experimental observation of isolated large transverse energy electrons with associated missing energy at $\sqrt{s} = 540$ GeV, Phys. Lett. B 122 (1983) 103, http://dx.doi.org/10.1016/0370-2693(83)91177-2.
[50] CMS Collaboration, Measurement of inclusive W and Z boson production cross sections in pp collisions at $\sqrt{s} = 8$ TeV, Phys. Rev. Lett. 112 (2014) 191802, http://dx.doi.org/10.1103/PhysRevLett.112.191802, arXiv:1402.0923.
[51] CMS Collaboration, Measurement of the polarization of W bosons with large transverse momenta in W + Jets events at the LHC, Phys. Rev. Lett. 107 (2011) 021802, http://dx.doi.org/10.1103/PhysRevLett.107.021802, arXiv:1104.3829.
[52] ATLAS Collaboration, Measurement of the polarisation of W bosons produced with large transverse momentum in pp collisions at $\sqrt{s} = 7$ TeV with the ATLAS experiment, Eur. Phys. J. C 72 (2012) 2001, http://dx.doi.org/10.1140/epjc/s10052-012-2001-6, arXiv:1203.2165.
[53] Z. Bern, G. Diana, L.J. Dixon, F. Febres Cordero, D. Forde, T. Gleisberg, S. Höche, H. Ita, D.A. Kosower, D. Maître, K. Ozeren, Left-handed W bosons at the LHC, Phys. Rev. D 84 (2011) 034008, http://dx.doi.org/10.1103/PhysRevD.84.034008, arXiv:1103.5445.
[54] CMS Collaboration, Measurement of the prompt J/ψ and $\psi(2S)$ polarizations in pp collisions at $\sqrt{s} = 7$ TeV, Phys. Lett. B 727 (2013) 381, http://dx.doi.org/10.1016/j.physletb.2013.10.055, arXiv:1307.6070.
[55] CMS Collaboration, Measurement of the properties of a Higgs boson in the four-lepton final state, Phys. Rev. D 89 (2014) 092007, http://dx.doi.org/10.1103/PhysRevD.89.092007, arXiv:1312.5353.
[56] ATLAS Collaboration, Measurement of spin correlation in top–antitop quark events and search for top squark pair production in pp collisions at $\sqrt{s} = 8$ TeV using the ATLAS detector, Phys. Rev. Lett. 114 (2015) 142001, http://dx.doi.org/10.1103/PhysRevLett.114.142001, arXiv:1412.4742.
[57] ATLAS Collaboration, Measurement of W^+W^- production in pp collisions at $\sqrt{s} = 7$ TeV with the ATLAS detector and limits on anomalous WWZ and WWγ couplings, Phys. Rev. D 87 (2013) 112001, http://dx.doi.org/10.1103/PhysRevD.87.112001, arXiv:1210.2979; Erratum: http://dx.doi.org/10.1103/PhysRevD.88.079906.
[58] CMS Collaboration, Measurement of the W^+W^- cross section in pp collisions at $\sqrt{s} = 8$ TeV and limits on anomalous gauge couplings, Eur. Phys. J. C (2016), submitted for publication, arXiv:1507.03268, 2015.
[59] CMS Collaboration, Measurement of WZ and ZZ production in pp collisions at $\sqrt{s} = 8$ TeV in final states with b-tagged jets, Eur. Phys. J. C 74 (2014) 2973, http://dx.doi.org/10.1140/epjc/s10052-014-2973-5, arXiv:1403.3047.
[60] T. Junk, Confidence level computation for combining searches with small statistics, Nucl. Instrum. Methods Phys. Res., Sect. A, Accel. Spectrom. Detect. Assoc. Equip. 434 (1999) 435, http://dx.doi.org/10.1016/S0168-9002(99)00498-2, arXiv:hep-ex/9902006.
[61] A.L. Read, Presentation of search results: the CL_s technique, J. Phys. G 28 (2002) 2693, http://dx.doi.org/10.1088/0954-3899/28/10/313.
[62] ATLAS and CMS Collaborations, LHC Higgs Combination Group, Procedure for the LHC Higgs boson search combination in Summer 2011, Technical Report ATL-PHYS-PUB/2011-11, CMS NOTE 2011/005, 2011, http://cdsweb.cern.ch/record/1379837.
[63] CMS Collaboration, CMS luminosity based on pixel cluster counting – summer 2013 update, CMS Physics Analysis Summary CMS-PAS-LUM-13-001, 2013, http://cdsweb.cern.ch/record/1598864.
[64] S. Alekhin, et al., The PDF4LHC working group interim report, arXiv:1101.0536, 2011.
[65] M. Botje, J. Butterworth, A. Cooper-Sarkar, A. de Roeck, J. Feltesse, S. Forte, A. Glazov, J. Huston, R. McNulty, T. Sjöstrand, R.S. Thorne, The PDF4LHC working group interim recommendations, arXiv:1101.0538, 2011.
[66] R.D. Ball, V. Bertone, S. Carrazza, C.S. Deans, L. Del Debbio, S. Forte, A. Guffanti, N.P. Hartland, J.I. Latorre, J. Rojo, M. Ubiali, NNPDF Collaboration, Parton distributions with LHC data, Nucl. Phys. B 867 (2013) 244, http://dx.doi.org/10.1016/j.nuclphysb.2012.10.003, arXiv:1207.1303.
[67] A.D. Martin, W.J. Stirling, R.S. Thorne, G. Watt, Parton distributions for the LHC, Eur. Phys. J. C 63 (2009) 189, http://dx.doi.org/10.1140/epjc/s10052-009-1072-5, arXiv:0901.0002.
[68] H.-L. Lai, M. Guzzi, J. Huston, Z. Li, P.M. Nadolsky, J. Pumplin, C.-P. Yuan, New parton distributions for collider physics, Phys. Rev. D 82 (2010) 074024, http://dx.doi.org/10.1103/PhysRevD.82.074024, arXiv:1007.2241.
[69] W. Beenakker, R. Höpker, M. Spira, P.M. Zerwas, Squark and gluino production at hadron colliders, Nucl. Phys. B 492 (1997) 51, http://dx.doi.org/10.1016/S0550-3213(97)80027-2, arXiv:hep-ph/9610490.
[70] A. Kulesza, L. Motyka, Threshold resummation for squark–antisquark and gluino-pair production at the LHC, Phys. Rev. Lett. 102 (2009) 111802, http://dx.doi.org/10.1103/PhysRevLett.102.111802, arXiv:0807.2405.
[71] A. Kulesza, L. Motyka, Soft gluon resummation for the production of gluino–gluino and squark–antisquark pairs at the LHC, Phys. Rev. D 80 (2009) 095004, http://dx.doi.org/10.1103/PhysRevD.80.095004, arXiv:0905.4749.
[72] W. Beenakker, S. Brensing, M. Krämer, A. Kulesza, E. Laenen, I. Niessen, Soft-gluon resummation for squark and gluino hadroproduction, J. High Energy Phys. 12 (2009) 041, http://dx.doi.org/10.1088/1126-6708/2009/12/041, arXiv:0909.4418.
[73] W. Beenakker, S. Brensing, M. Krämer, A. Kulesza, E. Laenen, L. Motyka, I. Niessen, Squark and gluino hadroproduction, Int. J. Mod. Phys. A 26 (2011) 2637, http://dx.doi.org/10.1142/S0217751X11053560, arXiv:1105.1110.
[74] M. Krämer, A. Kulesza, R. van der Leeuw, M. Mangano, S. Padhi, T. Plehn, X. Portell, Supersymmetry production cross sections in pp collisions at $\sqrt{s} = 7$ TeV, arXiv:1206.2892, 2012.
[75] B. Fuks, M. Klasen, D.R. Lamprea, M. Rothering, Gaugino production in proton–proton collisions at a center-of-mass energy of 8 TeV, J. High Energy Phys. 10 (2012) 081, http://dx.doi.org/10.1007/JHEP10(2012)081, arXiv:1207.2159.
[76] B. Fuks, M. Klasen, D.R. Lamprea, M. Rothering, Precision predictions for electroweak superpartner production at hadron colliders with Resummino, Eur. Phys. J. C 73 (2013) 2480, http://dx.doi.org/10.1140/epjc/s10052-013-2480-0, arXiv:1304.0790.
[77] B. Fuks, M. Klasen, D.R. Lamprea, M. Rothering, Revisiting slepton pair production at the Large Hadron Collider, J. High Energy Phys. 01 (2014) 168, http://dx.doi.org/10.1007/JHEP01(2014)168, arXiv:1310.2621.

CMS Collaboration

V. Khachatryan, A.M. Sirunyan, A. Tumasyan

Yerevan Physics Institute, Yerevan, Armenia

W. Adam, E. Asilar, T. Bergauer, J. Brandstetter, E. Brondolin, M. Dragicevic, J. Erö, M. Flechl, M. Friedl, R. Frühwirth [1], V.M. Ghete, C. Hartl, N. Hörmann, J. Hrubec, M. Jeitler [1], V. Knünz, A. König, M. Krammer [1], I. Krätschmer, D. Liko, T. Matsushita, I. Mikulec, D. Rabady [2], B. Rahbaran, H. Rohringer, J. Schieck [1], R. Schöfbeck, J. Strauss, W. Treberer-Treberspurg, W. Waltenberger, C.-E. Wulz [1]

Institut für Hochenergiephysik der OeAW, Wien, Austria

V. Mossolov, N. Shumeiko, J. Suarez Gonzalez

National Centre for Particle and High Energy Physics, Minsk, Belarus

S. Alderweireldt, T. Cornelis, E.A. De Wolf, X. Janssen, A. Knutsson, J. Lauwers, S. Luyckx, M. Van De Klundert, H. Van Haevermaet, P. Van Mechelen, N. Van Remortel, A. Van Spilbeeck

Universiteit Antwerpen, Antwerpen, Belgium

S. Abu Zeid, F. Blekman, J. D'Hondt, N. Daci, I. De Bruyn, K. Deroover, N. Heracleous, J. Keaveney, S. Lowette, L. Moreels, A. Olbrechts, Q. Python, D. Strom, S. Tavernier, W. Van Doninck, P. Van Mulders, G.P. Van Onsem, I. Van Parijs

Vrije Universiteit Brussel, Brussel, Belgium

P. Barria, H. Brun, C. Caillol, B. Clerbaux, G. De Lentdecker, G. Fasanella, L. Favart, A. Grebenyuk, G. Karapostoli, T. Lenzi, A. Léonard, T. Maerschalk, A. Marinov, L. Perniè, A. Randle-conde, T. Reis, T. Seva, C. Vander Velde, P. Vanlaer, R. Yonamine, F. Zenoni, F. Zhang [3]

Université Libre de Bruxelles, Bruxelles, Belgium

K. Beernaert, L. Benucci, A. Cimmino, S. Crucy, D. Dobur, A. Fagot, G. Garcia, M. Gul, J. Mccartin, A.A. Ocampo Rios, D. Poyraz, D. Ryckbosch, S. Salva, M. Sigamani, N. Strobbe, M. Tytgat, W. Van Driessche, E. Yazgan, N. Zaganidis

Ghent University, Ghent, Belgium

S. Basegmez, C. Beluffi [4], O. Bondu, S. Brochet, G. Bruno, A. Caudron, L. Ceard, G.G. Da Silveira, C. Delaere, D. Favart, L. Forthomme, A. Giammanco [5], J. Hollar, A. Jafari, P. Jez, M. Komm, V. Lemaitre, A. Mertens, M. Musich, C. Nuttens, L. Perrini, A. Pin, K. Piotrzkowski, A. Popov [6], L. Quertenmont, M. Selvaggi, M. Vidal Marono

Université Catholique de Louvain, Louvain-la-Neuve, Belgium

N. Beliy, G.H. Hammad

Université de Mons, Mons, Belgium

W.L. Aldá Júnior, F.L. Alves, G.A. Alves, L. Brito, M. Correa Martins Junior, M. Hamer, C. Hensel, C. Mora Herrera, A. Moraes, M.E. Pol, P. Rebello Teles

Centro Brasileiro de Pesquisas Fisicas, Rio de Janeiro, Brazil

E. Belchior Batista Das Chagas, W. Carvalho, J. Chinellato [7], A. Custódio, E.M. Da Costa, D. De Jesus Damiao, C. De Oliveira Martins, S. Fonseca De Souza, L.M. Huertas Guativa, H. Malbouisson, D. Matos Figueiredo, L. Mundim, H. Nogima, W.L. Prado Da Silva, A. Santoro, A. Sznajder, E.J. Tonelli Manganote [7], A. Vilela Pereira

Universidade do Estado do Rio de Janeiro, Rio de Janeiro, Brazil

S. Ahuja [a], C.A. Bernardes [b], A. De Souza Santos [b], S. Dogra [a], T.R. Fernandez Perez Tomei [a], E.M. Gregores [b], P.G. Mercadante [b], C.S. Moon [a,8], S.F. Novaes [a], Sandra S. Padula [a], D. Romero Abad, J.C. Ruiz Vargas

[a] *Universidade Estadual Paulista, São Paulo, Brazil*
[b] *Universidade Federal do ABC, São Paulo, Brazil*

A. Aleksandrov, R. Hadjiiska, P. Iaydjiev, M. Rodozov, S. Stoykova, G. Sultanov, M. Vutova

Institute for Nuclear Research and Nuclear Energy, Sofia, Bulgaria

A. Dimitrov, I. Glushkov, L. Litov, B. Pavlov, P. Petkov

University of Sofia, Sofia, Bulgaria

M. Ahmad, J.G. Bian, G.M. Chen, H.S. Chen, M. Chen, T. Cheng, R. Du, C.H. Jiang, R. Plestina [9], F. Romeo, S.M. Shaheen, A. Spiezia, J. Tao, C. Wang, Z. Wang, H. Zhang

Institute of High Energy Physics, Beijing, China

C. Asawatangtrakuldee, Y. Ban, Q. Li, S. Liu, Y. Mao, S.J. Qian, D. Wang, Z. Xu

State Key Laboratory of Nuclear Physics and Technology, Peking University, Beijing, China

C. Avila, A. Cabrera, L.F. Chaparro Sierra, C. Florez, J.P. Gomez, B. Gomez Moreno, J.C. Sanabria

Universidad de Los Andes, Bogota, Colombia

N. Godinovic, D. Lelas, I. Puljak, P.M. Ribeiro Cipriano

University of Split, Faculty of Electrical Engineering, Mechanical Engineering and Naval Architecture, Split, Croatia

Z. Antunovic, M. Kovac

University of Split, Faculty of Science, Split, Croatia

V. Brigljevic, K. Kadija, J. Luetic, S. Micanovic, L. Sudic

Institute Rudjer Boskovic, Zagreb, Croatia

A. Attikis, G. Mavromanolakis, J. Mousa, C. Nicolaou, F. Ptochos, P.A. Razis, H. Rykaczewski

University of Cyprus, Nicosia, Cyprus

M. Bodlak, M. Finger [10], M. Finger Jr. [10]

Charles University, Prague, Czech Republic

A.A. Abdelalim [11,12], A. Awad, M. El Sawy [13,14], A. Mahrous [11], A. Radi [14,15]

Academy of Scientific Research and Technology of the Arab Republic of Egypt, Egyptian Network of High Energy Physics, Cairo, Egypt

B. Calpas, M. Kadastik, M. Murumaa, M. Raidal, A. Tiko, C. Veelken

National Institute of Chemical Physics and Biophysics, Tallinn, Estonia

P. Eerola, J. Pekkanen, M. Voutilainen

Department of Physics, University of Helsinki, Helsinki, Finland

J. Härkönen, V. Karimäki, R. Kinnunen, T. Lampén, K. Lassila-Perini, S. Lehti, T. Lindén, P. Luukka, T. Mäenpää, T. Peltola, E. Tuominen, J. Tuominiemi, E. Tuovinen, L. Wendland

Helsinki Institute of Physics, Helsinki, Finland

J. Talvitie, T. Tuuva

Lappeenranta University of Technology, Lappeenranta, Finland

M. Besancon, F. Couderc, M. Dejardin, D. Denegri, B. Fabbro, J.L. Faure, C. Favaro, F. Ferri, S. Ganjour, A. Givernaud, P. Gras, G. Hamel de Monchenault, P. Jarry, E. Locci, M. Machet, J. Malcles, J. Rander, A. Rosowsky, M. Titov, A. Zghiche

DSM/IRFU, CEA/Saclay, Gif-sur-Yvette, France

I. Antropov, S. Baffioni, F. Beaudette, P. Busson, L. Cadamuro, E. Chapon, C. Charlot, T. Dahms, O. Davignon, N. Filipovic, A. Florent, R. Granier de Cassagnac, S. Lisniak, L. Mastrolorenzo, P. Miné, I.N. Naranjo, M. Nguyen, C. Ochando, G. Ortona, P. Paganini, P. Pigard, S. Regnard, R. Salerno, J.B. Sauvan, Y. Sirois, T. Strebler, Y. Yilmaz, A. Zabi

Laboratoire Leprince-Ringuet, Ecole Polytechnique, IN2P3–CNRS, Palaiseau, France

J.-L. Agram [16], J. Andrea, A. Aubin, D. Bloch, J.-M. Brom, M. Buttignol, E.C. Chabert, N. Chanon, C. Collard, E. Conte [16], X. Coubez, J.-C. Fontaine [16], D. Gelé, U. Goerlach, C. Goetzmann, A.-C. Le Bihan, J.A. Merlin [2], K. Skovpen, P. Van Hove

Institut Pluridisciplinaire Hubert Curien, Université de Strasbourg, Université de Haute Alsace Mulhouse, CNRS/IN2P3, Strasbourg, France

S. Gadrat

Centre de Calcul de l'Institut National de Physique Nucleaire et de Physique des Particules, CNRS/IN2P3, Villeurbanne, France

S. Beauceron, C. Bernet, G. Boudoul, E. Bouvier, C.A. Carrillo Montoya, R. Chierici, D. Contardo, B. Courbon, P. Depasse, H. El Mamouni, J. Fan, J. Fay, S. Gascon, M. Gouzevitch, B. Ille, F. Lagarde, I.B. Laktineh, M. Lethuillier, L. Mirabito, A.L. Pequegnot, S. Perries, J.D. Ruiz Alvarez, D. Sabes, L. Sgandurra, V. Sordini, M. Vander Donckt, P. Verdier, S. Viret

Université de Lyon, Université Claude Bernard Lyon 1, CNRS–IN2P3, Institut de Physique Nucléaire de Lyon, Villeurbanne, France

T. Toriashvili [17]

Georgian Technical University, Tbilisi, Georgia

Z. Tsamalaidze [10]

Tbilisi State University, Tbilisi, Georgia

C. Autermann, S. Beranek, M. Edelhoff, L. Feld, A. Heister, M.K. Kiesel, K. Klein, M. Lipinski, A. Ostapchuk, M. Preuten, F. Raupach, S. Schael, J.F. Schulte, T. Verlage, H. Weber, B. Wittmer, V. Zhukov [6]

RWTH Aachen University, I. Physikalisches Institut, Aachen, Germany

M. Ata, M. Brodski, E. Dietz-Laursonn, D. Duchardt, M. Endres, M. Erdmann, S. Erdweg, T. Esch, R. Fischer, A. Güth, T. Hebbeker, C. Heidemann, K. Hoepfner, D. Klingebiel, S. Knutzen, P. Kreuzer, M. Merschmeyer, A. Meyer, P. Millet, M. Olschewski, K. Padeken, P. Papacz, T. Pook, M. Radziej, H. Reithler, M. Rieger, F. Scheuch, L. Sonnenschein, D. Teyssier, S. Thüer

RWTH Aachen University, III. Physikalisches Institut A, Aachen, Germany

V. Cherepanov, Y. Erdogan, G. Flügge, H. Geenen, M. Geisler, F. Hoehle, B. Kargoll, T. Kress, Y. Kuessel, A. Künsken, J. Lingemann [2], A. Nehrkorn, A. Nowack, I.M. Nugent, C. Pistone, O. Pooth, A. Stahl

RWTH Aachen University, III. Physikalisches Institut B, Aachen, Germany

M. Aldaya Martin, I. Asin, N. Bartosik, O. Behnke, U. Behrens, A.J. Bell, K. Borras [18], A. Burgmeier, A. Campbell, S. Choudhury [19], F. Costanza, C. Diez Pardos, G. Dolinska, S. Dooling, T. Dorland, G. Eckerlin, D. Eckstein, T. Eichhorn, G. Flucke, E. Gallo [20], J. Garay Garcia, A. Geiser, A. Gizhko, P. Gunnellini, J. Hauk, M. Hempel [21], H. Jung, A. Kalogeropoulos, O. Karacheban [21], M. Kasemann, P. Katsas, J. Kieseler, C. Kleinwort, I. Korol, W. Lange, J. Leonard, K. Lipka, A. Lobanov, W. Lohmann [21], R. Mankel, I. Marfin [21], I.-A. Melzer-Pellmann, A.B. Meyer, G. Mittag, J. Mnich, A. Mussgiller, S. Naumann-Emme, A. Nayak, E. Ntomari, H. Perrey, D. Pitzl, R. Placakyte, A. Raspereza, B. Roland, M.Ö. Sahin, P. Saxena, T. Schoerner-Sadenius, M. Schröder, C. Seitz, S. Spannagel, K.D. Trippkewitz, R. Walsh, C. Wissing

Deutsches Elektronen-Synchrotron, Hamburg, Germany

V. Blobel, M. Centis Vignali, A.R. Draeger, J. Erfle, E. Garutti, K. Goebel, D. Gonzalez, M. Görner, J. Haller, M. Hoffmann, R.S. Höing, A. Junkes, R. Klanner, R. Kogler, T. Lapsien, T. Lenz, I. Marchesini, D. Marconi, M. Meyer, D. Nowatschin, J. Ott, F. Pantaleo [2], T. Peiffer, A. Perieanu, N. Pietsch, J. Poehlsen, D. Rathjens, C. Sander, H. Schettler, P. Schleper, E. Schlieckau, A. Schmidt, J. Schwandt, V. Sola, H. Stadie, G. Steinbrück, H. Tholen, D. Troendle, E. Usai, L. Vanelderen, A. Vanhoefer, B. Vormwald

University of Hamburg, Hamburg, Germany

M. Akbiyik, C. Barth, C. Baus, J. Berger, C. Böser, E. Butz, T. Chwalek, F. Colombo, W. De Boer, A. Descroix, A. Dierlamm, S. Fink, F. Frensch, R. Friese, M. Giffels, A. Gilbert, D. Haitz, F. Hartmann [2], S.M. Heindl, U. Husemann, I. Katkov [6], A. Kornmayer [2], P. Lobelle Pardo, B. Maier, H. Mildner, M.U. Mozer, T. Müller, Th. Müller, M. Plagge, G. Quast, K. Rabbertz, S. Röcker, F. Roscher, G. Sieber, H.J. Simonis, F.M. Stober, R. Ulrich, J. Wagner-Kuhr, S. Wayand, M. Weber, T. Weiler, C. Wöhrmann, R. Wolf

Institut für Experimentelle Kernphysik, Karlsruhe, Germany

G. Anagnostou, G. Daskalakis, T. Geralis, V.A. Giakoumopoulou, A. Kyriakis, D. Loukas, A. Psallidas, I. Topsis-Giotis

Institute of Nuclear and Particle Physics (INPP), NCSR Demokritos, Aghia Paraskevi, Greece

A. Agapitos, S. Kesisoglou, A. Panagiotou, N. Saoulidou, E. Tziaferi

National and Kapodistrian University of Athens, Athens, Greece

I. Evangelou, G. Flouris, C. Foudas, P. Kokkas, N. Loukas, N. Manthos, I. Papadopoulos, E. Paradas, J. Strologas

University of Ioánnina, Ioánnina, Greece

G. Bencze, C. Hajdu, A. Hazi, P. Hidas, D. Horvath [22], F. Sikler, V. Veszpremi, G. Vesztergombi [23], A.J. Zsigmond

Wigner Research Centre for Physics, Budapest, Hungary

N. Beni, S. Czellar, J. Karancsi [24], J. Molnar, Z. Szillasi

Institute of Nuclear Research ATOMKI, Debrecen, Hungary

M. Bartók [25], A. Makovec, P. Raics, Z.L. Trocsanyi, B. Ujvari

University of Debrecen, Debrecen, Hungary

P. Mal, K. Mandal, D.K. Sahoo, N. Sahoo, S.K. Swain

National Institute of Science Education and Research, Bhubaneswar, India

S. Bansal, S.B. Beri, V. Bhatnagar, R. Chawla, R. Gupta, U. Bhawandeep, A.K. Kalsi, A. Kaur, M. Kaur, R. Kumar, A. Mehta, M. Mittal, J.B. Singh, G. Walia

Panjab University, Chandigarh, India

Ashok Kumar, A. Bhardwaj, B.C. Choudhary, R.B. Garg, A. Kumar, S. Malhotra, M. Naimuddin, N. Nishu, K. Ranjan, R. Sharma, V. Sharma

University of Delhi, Delhi, India

S. Bhattacharya, K. Chatterjee, S. Dey, S. Dutta, Sa. Jain, N. Majumdar, A. Modak, K. Mondal, S. Mukherjee, S. Mukhopadhyay, A. Roy, D. Roy, S. Roy Chowdhury, S. Sarkar, M. Sharan

Saha Institute of Nuclear Physics, Kolkata, India

A. Abdulsalam, R. Chudasama, D. Dutta, V. Jha, V. Kumar, A.K. Mohanty [2], L.M. Pant, P. Shukla, A. Topkar

Bhabha Atomic Research Centre, Mumbai, India

T. Aziz, S. Banerjee, S. Bhowmik [26], R.M. Chatterjee, R.K. Dewanjee, S. Dugad, S. Ganguly, S. Ghosh, M. Guchait, A. Gurtu [27], G. Kole, S. Kumar, B. Mahakud, M. Maity [26], G. Majumder, K. Mazumdar, S. Mitra, G.B. Mohanty, B. Parida, T. Sarkar [26], N. Sur, B. Sutar, N. Wickramage [28]

Tata Institute of Fundamental Research, Mumbai, India

S. Chauhan, S. Dube, S. Sharma

Indian Institute of Science Education and Research (IISER), Pune, India

H. Bakhshiansohi, H. Behnamian, S.M. Etesami [29], A. Fahim [30], R. Goldouzian, M. Khakzad, M. Mohammadi Najafabadi, M. Naseri, S. Paktinat Mehdiabadi, F. Rezaei Hosseinabadi, B. Safarzadeh [31], M. Zeinali

Institute for Research in Fundamental Sciences (IPM), Tehran, Iran

M. Felcini, M. Grunewald

University College Dublin, Dublin, Ireland

M. Abbrescia [a,b], C. Calabria [a,b], C. Caputo [a,b], A. Colaleo [a], D. Creanza [a,c], L. Cristella [a,b], N. De Filippis [a,c], M. De Palma [a,b], L. Fiore [a], G. Iaselli [a,c], G. Maggi [a,c], M. Maggi [a], G. Miniello [a,b], S. My [a,c], S. Nuzzo [a,b], A. Pompili [a,b], G. Pugliese [a,c], R. Radogna [a,b], A. Ranieri [a], G. Selvaggi [a,b], L. Silvestris [a,2], R. Venditti [a,b], P. Verwilligen [a]

[a] *INFN Sezione di Bari, Bari, Italy*
[b] *Università di Bari, Bari, Italy*
[c] *Politecnico di Bari, Bari, Italy*

G. Abbiendi [a], C. Battilana [2], A.C. Benvenuti [a], D. Bonacorsi [a,b], S. Braibant-Giacomelli [a,b], L. Brigliadori [a,b], R. Campanini [a,b], P. Capiluppi [a,b], A. Castro [a,b], F.R. Cavallo [a], S.S. Chhibra [a,b], G. Codispoti [a,b], M. Cuffiani [a,b], G.M. Dallavalle [a], F. Fabbri [a], A. Fanfani [a,b], D. Fasanella [a,b], P. Giacomelli [a], C. Grandi [a], L. Guiducci [a,b], S. Marcellini [a], G. Masetti [a], A. Montanari [a], F.L. Navarria [a,b], A. Perrotta [a], A.M. Rossi [a,b], T. Rovelli [a,b], G.P. Siroli [a,b], N. Tosi [a,b], R. Travaglini [a,b]

[a] *INFN Sezione di Bologna, Bologna, Italy*
[b] *Università di Bologna, Bologna, Italy*

G. Cappello [a], M. Chiorboli [a,b], S. Costa [a,b], A. Di Mattia [a], F. Giordano [a,b], R. Potenza [a,b], A. Tricomi [a,b], C. Tuve [a,b]

[a] *INFN Sezione di Catania, Catania, Italy*
[b] *Università di Catania, Catania, Italy*

G. Barbagli [a], V. Ciulli [a,b], C. Civinini [a], R. D'Alessandro [a,b], E. Focardi [a,b], S. Gonzi [a,b], V. Gori [a,b], P. Lenzi [a,b], M. Meschini [a], S. Paoletti [a], G. Sguazzoni [a], A. Tropiano [a,b], L. Viliani [a,b,2]

[a] *INFN Sezione di Firenze, Firenze, Italy*
[b] *Università di Firenze, Firenze, Italy*

L. Benussi, S. Bianco, F. Fabbri, D. Piccolo, F. Primavera

INFN Laboratori Nazionali di Frascati, Frascati, Italy

V. Calvelli [a,b], F. Ferro [a], M. Lo Vetere [a,b], M.R. Monge [a,b], E. Robutti [a], S. Tosi [a,b]

[a] *INFN Sezione di Genova, Genova, Italy*
[b] *Università di Genova, Genova, Italy*

L. Brianza, M.E. Dinardo [a,b], S. Fiorendi [a,b], S. Gennai [a], R. Gerosa [a,b], A. Ghezzi [a,b], P. Govoni [a,b], S. Malvezzi [a], R.A. Manzoni [a,b], B. Marzocchi [a,b,2], D. Menasce [a], L. Moroni [a], M. Paganoni [a,b], D. Pedrini [a], S. Ragazzi [a,b], N. Redaelli [a], T. Tabarelli de Fatis [a,b]

[a] *INFN Sezione di Milano-Bicocca, Milano, Italy*
[b] *Università di Milano-Bicocca, Milano, Italy*

S. Buontempo [a], N. Cavallo [a,c], S. Di Guida [a,d,2], M. Esposito [a,b], F. Fabozzi [a,c], A.O.M. Iorio [a,b], G. Lanza [a], L. Lista [a], S. Meola [a,d,2], M. Merola [a], P. Paolucci [a,2], C. Sciacca [a,b], F. Thyssen

[a] *INFN Sezione di Napoli, Napoli, Italy*
[b] *Università di Napoli 'Federico II', Napoli, Italy*

[c] Università della Basilicata, Potenza, Italy
[d] Università G. Marconi, Roma, Italy

P. Azzi [a,2], N. Bacchetta [a], L. Benato [a,b], D. Bisello [a,b], A. Boletti [a,b], R. Carlin [a,b], P. Checchia [a], M. Dall'Osso [a,b,2], T. Dorigo [a], U. Dosselli [a], F. Gasparini [a,b], U. Gasparini [a,b], A. Gozzelino [a], S. Lacaprara [a], M. Margoni [a,b], A.T. Meneguzzo [a,b], M. Passaseo [a], J. Pazzini [a,b], M. Pegoraro [a], N. Pozzobon [a,b], P. Ronchese [a,b], F. Simonetto [a,b], E. Torassa [a], M. Tosi [a,b], S. Vanini [a,b], M. Zanetti, P. Zotto [a,b], A. Zucchetta [a,b,2], G. Zumerle [a,b]

[a] INFN Sezione di Padova, Padova, Italy
[b] Università di Padova, Padova, Italy
[c] Università di Trento, Trento, Italy

A. Braghieri [a], A. Magnani [a], P. Montagna [a,b], S.P. Ratti [a,b], V. Re [a], C. Riccardi [a,b], P. Salvini [a], I. Vai [a], P. Vitulo [a,b]

[a] INFN Sezione di Pavia, Pavia, Italy
[b] Università di Pavia, Pavia, Italy

L. Alunni Solestizi [a,b], M. Biasini [a,b], G.M. Bilei [a], D. Ciangottini [a,b,2], L. Fanò [a,b], P. Lariccia [a,b], G. Mantovani [a,b], M. Menichelli [a], A. Saha [a], A. Santocchia [a,b]

[a] INFN Sezione di Perugia, Perugia, Italy
[b] Università di Perugia, Perugia, Italy

K. Androsov [a,32], P. Azzurri [a], G. Bagliesi [a], J. Bernardini [a], T. Boccali [a], R. Castaldi [a], M.A. Ciocci [a,32], R. Dell'Orso [a], S. Donato [a,c,2], G. Fedi, L. Foà [a,c,†], A. Giassi [a], M.T. Grippo [a,32], F. Ligabue [a,c], T. Lomtadze [a], L. Martini [a,b], A. Messineo [a,b], F. Palla [a], A. Rizzi [a,b], A. Savoy-Navarro [a,33], A.T. Serban [a], P. Spagnolo [a], R. Tenchini [a], G. Tonelli [a,b], A. Venturi [a], P.G. Verdini [a]

[a] INFN Sezione di Pisa, Pisa, Italy
[b] Università di Pisa, Pisa, Italy
[c] Scuola Normale Superiore di Pisa, Pisa, Italy

L. Barone [a,b], F. Cavallari [a], G. D'imperio [a,b,2], D. Del Re [a,b], M. Diemoz [a], S. Gelli [a,b], C. Jorda [a], E. Longo [a,b], F. Margaroli [a,b], P. Meridiani [a], G. Organtini [a,b], R. Paramatti [a], F. Preiato [a,b], S. Rahatlou [a,b], C. Rovelli [a], F. Santanastasio [a,b], P. Traczyk [a,b,2]

[a] INFN Sezione di Roma, Roma, Italy
[b] Università di Roma, Roma, Italy

N. Amapane [a,b], R. Arcidiacono [a,c,2], S. Argiro [a,b], M. Arneodo [a,c], R. Bellan [a,b], C. Biino [a], N. Cartiglia [a], M. Costa [a,b], R. Covarelli [a,b], A. Degano [a,b], N. Demaria [a], L. Finco [a,b,2], B. Kiani [a,b], C. Mariotti [a], S. Maselli [a], E. Migliore [a,b], V. Monaco [a,b], E. Monteil [a,b], M.M. Obertino [a,b], L. Pacher [a,b], N. Pastrone [a], M. Pelliccioni [a], G.L. Pinna Angioni [a,b], F. Ravera [a,b], A. Romero [a,b], M. Ruspa [a,c], R. Sacchi [a,b], A. Solano [a,b], A. Staiano [a], U. Tamponi [a]

[a] INFN Sezione di Torino, Torino, Italy
[b] Università di Torino, Torino, Italy
[c] Università del Piemonte Orientale, Novara, Italy

S. Belforte [a], V. Candelise [a,b,2], M. Casarsa [a], F. Cossutti [a], G. Della Ricca [a,b], B. Gobbo [a], C. La Licata [a,b], M. Marone [a,b], A. Schizzi [a,b], A. Zanetti [a]

[a] INFN Sezione di Trieste, Trieste, Italy
[b] Università di Trieste, Trieste, Italy

A. Kropivnitskaya, S.K. Nam

Kangwon National University, Chunchon, Republic of Korea

D.H. Kim, G.N. Kim, M.S. Kim, D.J. Kong, S. Lee, Y.D. Oh, A. Sakharov, D.C. Son

Kyungpook National University, Daegu, Republic of Korea

J.A. Brochero Cifuentes, H. Kim, T.J. Kim

Chonbuk National University, Jeonju, Republic of Korea

S. Song

Chonnam National University, Institute for Universe and Elementary Particles, Kwangju, Republic of Korea

S. Choi, Y. Go, D. Gyun, B. Hong, M. Jo, H. Kim, Y. Kim, B. Lee, K. Lee, K.S. Lee, S. Lee, S.K. Park, Y. Roh

Korea University, Seoul, Republic of Korea

H.D. Yoo

Seoul National University, Seoul, Republic of Korea

M. Choi, H. Kim, J.H. Kim, J.S.H. Lee, I.C. Park, G. Ryu, M.S. Ryu

University of Seoul, Seoul, Republic of Korea

Y. Choi, J. Goh, D. Kim, E. Kwon, J. Lee, I. Yu

Sungkyunkwan University, Suwon, Republic of Korea

A. Juodagalvis, J. Vaitkus

Vilnius University, Vilnius, Lithuania

I. Ahmed, Z.A. Ibrahim, J.R. Komaragiri, M.A.B. Md Ali [34], F. Mohamad Idris [35], W.A.T. Wan Abdullah, M.N. Yusli

National Centre for Particle Physics, Universiti Malaya, Kuala Lumpur, Malaysia

E. Casimiro Linares, H. Castilla-Valdez, E. De La Cruz-Burelo, I. Heredia-De La Cruz [36], A. Hernandez-Almada, R. Lopez-Fernandez, A. Sanchez-Hernandez

Centro de Investigacion y de Estudios Avanzados del IPN, Mexico City, Mexico

S. Carrillo Moreno, F. Vazquez Valencia

Universidad Iberoamericana, Mexico City, Mexico

I. Pedraza, H.A. Salazar Ibarguen

Benemerita Universidad Autonoma de Puebla, Puebla, Mexico

A. Morelos Pineda

Universidad Autónoma de San Luis Potosí, San Luis Potosí, Mexico

D. Krofcheck

University of Auckland, Auckland, New Zealand

P.H. Butler

University of Canterbury, Christchurch, New Zealand

A. Ahmad, M. Ahmad, Q. Hassan, H.R. Hoorani, W.A. Khan, T. Khurshid, M. Shoaib

National Centre for Physics, Quaid-I-Azam University, Islamabad, Pakistan

H. Bialkowska, M. Bluj, B. Boimska, T. Frueboes, M. Górski, M. Kazana, K. Nawrocki, K. Romanowska-Rybinska, M. Szleper, P. Zalewski

National Centre for Nuclear Research, Swierk, Poland

G. Brona, K. Bunkowski, A. Byszuk [37], K. Doroba, A. Kalinowski, M. Konecki, J. Krolikowski, M. Misiura, M. Olszewski, M. Walczak

Institute of Experimental Physics, Faculty of Physics, University of Warsaw, Warsaw, Poland

P. Bargassa, C. Beirão Da Cruz E Silva, A. Di Francesco, P. Faccioli, P.G. Ferreira Parracho, M. Gallinaro, N. Leonardo, L. Lloret Iglesias, F. Nguyen, J. Rodrigues Antunes, J. Seixas, O. Toldaiev, D. Vadruccio, J. Varela, P. Vischia

Laboratório de Instrumentação e Física Experimental de Partículas, Lisboa, Portugal

S. Afanasiev, P. Bunin, M. Gavrilenko, I. Golutvin, I. Gorbunov, A. Kamenev, V. Karjavin, V. Konoplyanikov, A. Lanev, A. Malakhov, V. Matveev [38], P. Moisenz, V. Palichik, V. Perelygin, S. Shmatov, S. Shulha, N. Skatchkov, V. Smirnov, A. Zarubin

Joint Institute for Nuclear Research, Dubna, Russia

V. Golovtsov, Y. Ivanov, V. Kim [39], E. Kuznetsova, P. Levchenko, V. Murzin, V. Oreshkin, I. Smirnov, V. Sulimov, L. Uvarov, S. Vavilov, A. Vorobyev

Petersburg Nuclear Physics Institute, Gatchina (St. Petersburg), Russia

Yu. Andreev, A. Dermenev, S. Gninenko, N. Golubev, A. Karneyeu, M. Kirsanov, N. Krasnikov, A. Pashenkov, D. Tlisov, A. Toropin

Institute for Nuclear Research, Moscow, Russia

V. Epshteyn, V. Gavrilov, N. Lychkovskaya, V. Popov, I. Pozdnyakov, G. Safronov, A. Spiridonov, E. Vlasov, A. Zhokin

Institute for Theoretical and Experimental Physics, Moscow, Russia

A. Bylinkin

National Research Nuclear University 'Moscow Engineering Physics Institute' (MEPhI), Moscow, Russia

V. Andreev, M. Azarkin [40], I. Dremin [40], M. Kirakosyan, A. Leonidov [40], G. Mesyats, S.V. Rusakov

P.N. Lebedev Physical Institute, Moscow, Russia

A. Baskakov, A. Belyaev, E. Boos, M. Dubinin [41], L. Dudko, A. Ershov, A. Gribushin, V. Klyukhin, O. Kodolova, I. Lokhtin, I. Myagkov, S. Obraztsov, S. Petrushanko, V. Savrin, A. Snigirev

Skobeltsyn Institute of Nuclear Physics, Lomonosov Moscow State University, Moscow, Russia

I. Azhgirey, I. Bayshev, S. Bitioukov, V. Kachanov, A. Kalinin, D. Konstantinov, V. Krychkine, V. Petrov, R. Ryutin, A. Sobol, L. Tourtchanovitch, S. Troshin, N. Tyurin, A. Uzunian, A. Volkov

State Research Center of Russian Federation, Institute for High Energy Physics, Protvino, Russia

P. Adzic [42], J. Milosevic, V. Rekovic

University of Belgrade, Faculty of Physics and Vinca Institute of Nuclear Sciences, Belgrade, Serbia

J. Alcaraz Maestre, E. Calvo, M. Cerrada, M. Chamizo Llatas, N. Colino, B. De La Cruz, A. Delgado Peris, D. Domínguez Vázquez, A. Escalante Del Valle, C. Fernandez Bedoya, J.P. Fernández Ramos, J. Flix, M.C. Fouz, P. Garcia-Abia, O. Gonzalez Lopez, S. Goy Lopez, J.M. Hernandez, M.I. Josa, E. Navarro De Martino, A. Pérez-Calero Yzquierdo, J. Puerta Pelayo, A. Quintario Olmeda, I. Redondo, L. Romero, J. Santaolalla, M.S. Soares

Centro de Investigaciones Energéticas Medioambientales y Tecnológicas (CIEMAT), Madrid, Spain

C. Albajar, J.F. de Trocóniz, M. Missiroli, D. Moran

Universidad Autónoma de Madrid, Madrid, Spain

J. Cuevas, J. Fernandez Menendez, S. Folgueras, I. Gonzalez Caballero, E. Palencia Cortezon, J.M. Vizan Garcia

Universidad de Oviedo, Oviedo, Spain

I.J. Cabrillo, A. Calderon, J.R. Castiñeiras De Saa, P. De Castro Manzano, J. Duarte Campderros, M. Fernandez, J. Garcia-Ferrero, G. Gomez, A. Lopez Virto, J. Marco, R. Marco, C. Martinez Rivero, F. Matorras, F.J. Munoz Sanchez, J. Piedra Gomez, T. Rodrigo, A.Y. Rodríguez-Marrero, A. Ruiz-Jimeno, L. Scodellaro, N. Trevisani, I. Vila, R. Vilar Cortabitarte

Instituto de Física de Cantabria (IFCA), CSIC–Universidad de Cantabria, Santander, Spain

D. Abbaneo, E. Auffray, G. Auzinger, M. Bachtis, P. Baillon, A.H. Ball, D. Barney, A. Benaglia, J. Bendavid, L. Benhabib, J.F. Benitez, G.M. Berruti, P. Bloch, A. Bocci, A. Bonato, C. Botta, H. Breuker, T. Camporesi, R. Castello, G. Cerminara, M. D'Alfonso, D. d'Enterria, A. Dabrowski, V. Daponte, A. David, M. De Gruttola, F. De Guio, A. De Roeck, S. De Visscher, E. Di Marco, M. Dobson, M. Dordevic, B. Dorney, T. du Pree, M. Dünser, N. Dupont, A. Elliott-Peisert, G. Franzoni, W. Funk, D. Gigi, K. Gill, D. Giordano, M. Girone, F. Glege, R. Guida, S. Gundacker, M. Guthoff, J. Hammer, P. Harris, J. Hegeman, V. Innocente, P. Janot, H. Kirschenmann, M.J. Kortelainen, K. Kousouris, K. Krajczar, P. Lecoq, C. Lourenço, M.T. Lucchini, N. Magini, L. Malgeri, M. Mannelli, A. Martelli, L. Masetti, F. Meijers, S. Mersi, E. Meschi, F. Moortgat, S. Morovic, M. Mulders, M.V. Nemallapudi, H. Neugebauer, S. Orfanelli [43], L. Orsini, L. Pape, E. Perez, M. Peruzzi, A. Petrilli, G. Petrucciani, A. Pfeiffer, D. Piparo, A. Racz, G. Rolandi [44], M. Rovere, M. Ruan, H. Sakulin, C. Schäfer, C. Schwick, M. Seidel, A. Sharma, P. Silva, M. Simon, P. Sphicas [45], J. Steggemann, B. Stieger, M. Stoye, Y. Takahashi, D. Treille, A. Triossi, A. Tsirou, G.I. Veres [23], N. Wardle, H.K. Wöhri, A. Zagozdzinska [37], W.D. Zeuner

CERN, European Organization for Nuclear Research, Geneva, Switzerland

W. Bertl, K. Deiters, W. Erdmann, R. Horisberger, Q. Ingram, H.C. Kaestli, D. Kotlinski, U. Langenegger, D. Renker, T. Rohe

Paul Scherrer Institut, Villigen, Switzerland

F. Bachmair, L. Bäni, L. Bianchini, B. Casal, G. Dissertori, M. Dittmar, M. Donegà, P. Eller, C. Grab, C. Heidegger, D. Hits, J. Hoss, G. Kasieczka, W. Lustermann, B. Mangano, M. Marionneau, P. Martinez Ruiz del Arbol, M. Masciovecchio, D. Meister, F. Micheli, P. Musella, F. Nessi-Tedaldi, F. Pandolfi, J. Pata, F. Pauss, L. Perrozzi, M. Quittnat, M. Rossini, A. Starodumov [46], M. Takahashi, V.R. Tavolaro, K. Theofilatos, R. Wallny

Institute for Particle Physics, ETH Zurich, Zurich, Switzerland

T.K. Aarrestad, C. Amsler [47], L. Caminada, M.F. Canelli, V. Chiochia, A. De Cosa, C. Galloni, A. Hinzmann, T. Hreus, B. Kilminster, C. Lange, J. Ngadiuba, D. Pinna, P. Robmann, F.J. Ronga, D. Salerno, Y. Yang

Universität Zürich, Zurich, Switzerland

M. Cardaci, K.H. Chen, T.H. Doan, Sh. Jain, R. Khurana, M. Konyushikhin, C.M. Kuo, W. Lin, Y.J. Lu, S.S. Yu

National Central University, Chung-Li, Taiwan

Arun Kumar, R. Bartek, P. Chang, Y.H. Chang, Y.W. Chang, Y. Chao, K.F. Chen, P.H. Chen, C. Dietz, F. Fiori, U. Grundler, W.-S. Hou, Y. Hsiung, Y.F. Liu, R.-S. Lu, M. Miñano Moya, E. Petrakou, J.f. Tsai, Y.M. Tzeng

National Taiwan University (NTU), Taipei, Taiwan

B. Asavapibhop, K. Kovitanggoon, G. Singh, N. Srimanobhas, N. Suwonjandee

Chulalongkorn University, Faculty of Science, Department of Physics, Bangkok, Thailand

A. Adiguzel, M.N. Bakirci [48], Z.S. Demiroglu, C. Dozen, S. Girgis, G. Gokbulut, Y. Guler, E. Gurpinar, I. Hos, E.E. Kangal [49], A. Kayis Topaksu, G. Onengut [50], K. Ozdemir [51], S. Ozturk [48], D. Sunar Cerci [52], B. Tali [52], H. Topakli [48], M. Vergili, C. Zorbilmez

Cukurova University, Adana, Turkey

I.V. Akin, B. Bilin, S. Bilmis, B. Isildak [53], G. Karapinar [54], M. Yalvac, M. Zeyrek

Middle East Technical University, Physics Department, Ankara, Turkey

E. Gülmez, M. Kaya [55], O. Kaya [56], E.A. Yetkin [57], T. Yetkin [58]

Bogazici University, Istanbul, Turkey

A. Cakir, K. Cankocak, S. Sen [59], F.I. Vardarlı

Istanbul Technical University, Istanbul, Turkey

B. Grynyov

Institute for Scintillation Materials of National Academy of Science of Ukraine, Kharkov, Ukraine

L. Levchuk, P. Sorokin

National Scientific Center, Kharkov Institute of Physics and Technology, Kharkov, Ukraine

R. Aggleton, F. Ball, L. Beck, J.J. Brooke, E. Clement, D. Cussans, H. Flacher, J. Goldstein, M. Grimes, G.P. Heath, H.F. Heath, J. Jacob, L. Kreczko, C. Lucas, Z. Meng, D.M. Newbold [60], S. Paramesvaran, A. Poll, T. Sakuma, S. Seif El Nasr-storey, S. Senkin, D. Smith, V.J. Smith

University of Bristol, Bristol, United Kingdom

K.W. Bell, A. Belyaev [61], C. Brew, R.M. Brown, L. Calligaris, D. Cieri, D.J.A. Cockerill, J.A. Coughlan, K. Harder, S. Harper, E. Olaiya, D. Petyt, C.H. Shepherd-Themistocleous, A. Thea, I.R. Tomalin, T. Williams, W.J. Womersley, S.D. Worm

Rutherford Appleton Laboratory, Didcot, United Kingdom

M. Baber, R. Bainbridge, O. Buchmuller, A. Bundock, D. Burton, S. Casasso, M. Citron, D. Colling, L. Corpe, N. Cripps, P. Dauncey, G. Davies, A. De Wit, M. Della Negra, P. Dunne, A. Elwood, W. Ferguson, J. Fulcher, D. Futyan, G. Hall, G. Iles, M. Kenzie, R. Lane, R. Lucas [60], L. Lyons, A.-M. Magnan, S. Malik, J. Nash, A. Nikitenko [46], J. Pela, M. Pesaresi, K. Petridis, D.M. Raymond, A. Richards, A. Rose, C. Seez, A. Tapper, K. Uchida, M. Vazquez Acosta [62], T. Virdee, S.C. Zenz

Imperial College, London, United Kingdom

J.E. Cole, P.R. Hobson, A. Khan, P. Kyberd, D. Leggat, D. Leslie, I.D. Reid, P. Symonds, L. Teodorescu, M. Turner

Brunel University, Uxbridge, United Kingdom

A. Borzou, K. Call, J. Dittmann, K. Hatakeyama, H. Liu, N. Pastika

Baylor University, Waco, USA

O. Charaf, S.I. Cooper, C. Henderson, P. Rumerio

The University of Alabama, Tuscaloosa, USA

D. Arcaro, A. Avetisyan, T. Bose, C. Fantasia, D. Gastler, P. Lawson, D. Rankin, C. Richardson, J. Rohlf, J. St. John, L. Sulak, D. Zou

Boston University, Boston, USA

J. Alimena, E. Berry, S. Bhattacharya, D. Cutts, N. Dhingra, A. Ferapontov, A. Garabedian, J. Hakala, U. Heintz, E. Laird, G. Landsberg, Z. Mao, M. Narain, S. Piperov, S. Sagir, R. Syarif

Brown University, Providence, USA

R. Breedon, G. Breto, M. Calderon De La Barca Sanchez, S. Chauhan, M. Chertok, J. Conway, R. Conway, P.T. Cox, R. Erbacher, M. Gardner, W. Ko, R. Lander, M. Mulhearn, D. Pellett, J. Pilot, F. Ricci-Tam, S. Shalhout, J. Smith, M. Squires, D. Stolp, M. Tripathi, S. Wilbur, R. Yohay

University of California, Davis, Davis, USA

R. Cousins, P. Everaerts, C. Farrell, J. Hauser, M. Ignatenko, D. Saltzberg, E. Takasugi, V. Valuev, M. Weber

University of California, Los Angeles, USA

K. Burt, R. Clare, J. Ellison, J.W. Gary, G. Hanson, J. Heilman, M. Ivova Paneva, P. Jandir, E. Kennedy, F. Lacroix, O.R. Long, A. Luthra, M. Malberti, M. Olmedo Negrete, A. Shrinivas, H. Wei, S. Wimpenny, B.R. Yates

University of California, Riverside, Riverside, USA

J.G. Branson, G.B. Cerati, S. Cittolin, R.T. D'Agnolo, M. Derdzinski, A. Holzner, R. Kelley, D. Klein, J. Letts, I. Macneill, D. Olivito, S. Padhi, M. Pieri, M. Sani, V. Sharma, S. Simon, M. Tadel, A. Vartak, S. Wasserbaech [63], C. Welke, F. Würthwein, A. Yagil, G. Zevi Della Porta

University of California, San Diego, La Jolla, USA

J. Bradmiller-Feld, C. Campagnari, A. Dishaw, V. Dutta, K. Flowers, M. Franco Sevilla, P. Geffert, C. George, F. Golf, L. Gouskos, J. Gran, J. Incandela, N. Mccoll, S.D. Mullin, J. Richman, D. Stuart, I. Suarez, C. West, J. Yoo

University of California, Santa Barbara, Santa Barbara, USA

D. Anderson, A. Apresyan, A. Bornheim, J. Bunn, Y. Chen, J. Duarte, A. Mott, H.B. Newman, C. Pena, M. Pierini, M. Spiropulu, J.R. Vlimant, S. Xie, R.Y. Zhu

California Institute of Technology, Pasadena, USA

M.B. Andrews, V. Azzolini, A. Calamba, B. Carlson, T. Ferguson, M. Paulini, J. Russ, M. Sun, H. Vogel, I. Vorobiev

Carnegie Mellon University, Pittsburgh, USA

J.P. Cumalat, W.T. Ford, A. Gaz, F. Jensen, A. Johnson, M. Krohn, T. Mulholland, U. Nauenberg, K. Stenson, S.R. Wagner

University of Colorado Boulder, Boulder, USA

J. Alexander, A. Chatterjee, J. Chaves, J. Chu, S. Dittmer, N. Eggert, N. Mirman, G. Nicolas Kaufman, J.R. Patterson, A. Rinkevicius, A. Ryd, L. Skinnari, L. Soffi, W. Sun, S.M. Tan, W.D. Teo, J. Thom, J. Thompson, J. Tucker, Y. Weng, P. Wittich

Cornell University, Ithaca, USA

S. Abdullin, M. Albrow, J. Anderson, G. Apollinari, S. Banerjee, L.A.T. Bauerdick, A. Beretvas, J. Berryhill, P.C. Bhat, G. Bolla, K. Burkett, J.N. Butler, H.W.K. Cheung, F. Chlebana, S. Cihangir, V.D. Elvira, I. Fisk, J. Freeman, E. Gottschalk, L. Gray, D. Green, S. Grünendahl, O. Gutsche, J. Hanlon, D. Hare, R.M. Harris,

S. Hasegawa, J. Hirschauer, Z. Hu, S. Jindariani, M. Johnson, U. Joshi, A.W. Jung, B. Klima, B. Kreis, S. Kwan [†], S. Lammel, J. Linacre, D. Lincoln, R. Lipton, T. Liu, R. Lopes De Sá, J. Lykken, K. Maeshima, J.M. Marraffino, V.I. Martinez Outschoorn, S. Maruyama, D. Mason, P. McBride, P. Merkel, K. Mishra, S. Mrenna, S. Nahn, C. Newman-Holmes, V. O'Dell, K. Pedro, O. Prokofyev, G. Rakness, E. Sexton-Kennedy, A. Soha, W.J. Spalding, L. Spiegel, L. Taylor, S. Tkaczyk, N.V. Tran, L. Uplegger, E.W. Vaandering, C. Vernieri, M. Verzocchi, R. Vidal, H.A. Weber, A. Whitbeck, F. Yang

Fermi National Accelerator Laboratory, Batavia, USA

D. Acosta, P. Avery, P. Bortignon, D. Bourilkov, A. Carnes, M. Carver, D. Curry, S. Das, G.P. Di Giovanni, R.D. Field, I.K. Furic, S.V. Gleyzer, J. Hugon, J. Konigsberg, A. Korytov, J.F. Low, P. Ma, K. Matchev, H. Mei, P. Milenovic [64], G. Mitselmakher, D. Rank, R. Rossin, L. Shchutska, M. Snowball, D. Sperka, N. Terentyev, L. Thomas, J. Wang, S. Wang, J. Yelton

University of Florida, Gainesville, USA

S. Hewamanage, S. Linn, P. Markowitz, G. Martinez, J.L. Rodriguez

Florida International University, Miami, USA

A. Ackert, J.R. Adams, T. Adams, A. Askew, J. Bochenek, B. Diamond, J. Haas, S. Hagopian, V. Hagopian, K.F. Johnson, A. Khatiwada, H. Prosper, M. Weinberg

Florida State University, Tallahassee, USA

M.M. Baarmand, V. Bhopatkar, S. Colafranceschi [65], M. Hohlmann, H. Kalakhety, D. Noonan, T. Roy, F. Yumiceva

Florida Institute of Technology, Melbourne, USA

M.R. Adams, L. Apanasevich, D. Berry, R.R. Betts, I. Bucinskaite, R. Cavanaugh, O. Evdokimov, L. Gauthier, C.E. Gerber, D.J. Hofman, P. Kurt, C. O'Brien, I.D. Sandoval Gonzalez, C. Silkworth, P. Turner, N. Varelas, Z. Wu, M. Zakaria

University of Illinois at Chicago (UIC), Chicago, USA

B. Bilki [66], W. Clarida, K. Dilsiz, S. Durgut, R.P. Gandrajula, M. Haytmyradov, V. Khristenko, J.-P. Merlo, H. Mermerkaya [67], A. Mestvirishvili, A. Moeller, J. Nachtman, H. Ogul, Y. Onel, F. Ozok [57], A. Penzo, C. Snyder, E. Tiras, J. Wetzel, K. Yi

The University of Iowa, Iowa City, USA

I. Anderson, B.A. Barnett, B. Blumenfeld, N. Eminizer, D. Fehling, L. Feng, A.V. Gritsan, P. Maksimovic, C. Martin, M. Osherson, J. Roskes, A. Sady, U. Sarica, M. Swartz, M. Xiao, Y. Xin, C. You

Johns Hopkins University, Baltimore, USA

P. Baringer, A. Bean, G. Benelli, C. Bruner, R.P. Kenny III, D. Majumder, M. Malek, M. Murray, S. Sanders, R. Stringer, Q. Wang

The University of Kansas, Lawrence, USA

A. Ivanov, K. Kaadze, S. Khalil, M. Makouski, Y. Maravin, A. Mohammadi, L.K. Saini, N. Skhirtladze, S. Toda

Kansas State University, Manhattan, USA

D. Lange, F. Rebassoo, D. Wright

Lawrence Livermore National Laboratory, Livermore, USA

C. Anelli, A. Baden, O. Baron, A. Belloni, B. Calvert, S.C. Eno, C. Ferraioli, J.A. Gomez, N.J. Hadley, S. Jabeen, R.G. Kellogg, T. Kolberg, J. Kunkle, Y. Lu, A.C. Mignerey, Y.H. Shin, A. Skuja, M.B. Tonjes, S.C. Tonwar

University of Maryland, College Park, USA

A. Apyan, R. Barbieri, A. Baty, K. Bierwagen, S. Brandt, W. Busza, I.A. Cali, Z. Demiragli, L. Di Matteo, G. Gomez Ceballos, M. Goncharov, D. Gulhan, Y. Iiyama, G.M. Innocenti, M. Klute, D. Kovalskyi, Y.S. Lai, Y.-J. Lee, A. Levin, P.D. Luckey, A.C. Marini, C. Mcginn, C. Mironov, S. Narayanan, X. Niu, C. Paus, D. Ralph, C. Roland, G. Roland, J. Salfeld-Nebgen, G.S.F. Stephans, K. Sumorok, M. Varma, D. Velicanu, J. Veverka, J. Wang, T.W. Wang, B. Wyslouch, M. Yang, V. Zhukova

Massachusetts Institute of Technology, Cambridge, USA

B. Dahmes, A. Evans, A. Finkel, A. Gude, P. Hansen, S. Kalafut, S.C. Kao, K. Klapoetke, Y. Kubota, Z. Lesko, J. Mans, S. Nourbakhsh, N. Ruckstuhl, R. Rusack, N. Tambe, J. Turkewitz

University of Minnesota, Minneapolis, USA

J.G. Acosta, S. Oliveros

University of Mississippi, Oxford, USA

E. Avdeeva, K. Bloom, S. Bose, D.R. Claes, A. Dominguez, C. Fangmeier, R. Gonzalez Suarez, R. Kamalieddin, J. Keller, D. Knowlton, I. Kravchenko, J. Lazo-Flores, F. Meier, J. Monroy, F. Ratnikov, J.E. Siado, G.R. Snow

University of Nebraska–Lincoln, Lincoln, USA

M. Alyari, J. Dolen, J. George, A. Godshalk, C. Harrington, I. Iashvili, J. Kaisen, A. Kharchilava, A. Kumar, S. Rappoccio, B. Roozbahani

State University of New York at Buffalo, Buffalo, USA

G. Alverson, E. Barberis, D. Baumgartel, M. Chasco, A. Hortiangtham, A. Massironi, D.M. Morse, D. Nash, T. Orimoto, R. Teixeira De Lima, D. Trocino, R.-J. Wang, D. Wood, J. Zhang

Northeastern University, Boston, USA

K.A. Hahn, A. Kubik, N. Mucia, N. Odell, B. Pollack, A. Pozdnyakov, M. Schmitt, S. Stoynev, K. Sung, M. Trovato, M. Velasco

Northwestern University, Evanston, USA

A. Brinkerhoff, N. Dev, M. Hildreth, C. Jessop, D.J. Karmgard, N. Kellams, K. Lannon, S. Lynch, N. Marinelli, F. Meng, C. Mueller, Y. Musienko [38], T. Pearson, M. Planer, A. Reinsvold, R. Ruchti, G. Smith, S. Taroni, N. Valls, M. Wayne, M. Wolf, A. Woodard

University of Notre Dame, Notre Dame, USA

L. Antonelli, J. Brinson, B. Bylsma, L.S. Durkin, S. Flowers, A. Hart, C. Hill, R. Hughes, W. Ji, K. Kotov, T.Y. Ling, B. Liu, W. Luo, D. Puigh, M. Rodenburg, B.L. Winer, H.W. Wulsin

The Ohio State University, Columbus, USA

O. Driga, P. Elmer, J. Hardenbrook, P. Hebda, S.A. Koay, P. Lujan, D. Marlow, T. Medvedeva, M. Mooney, J. Olsen, C. Palmer, P. Piroué, X. Quan, H. Saka, D. Stickland, C. Tully, J.S. Werner, A. Zuranski

Princeton University, Princeton, USA

S. Malik

University of Puerto Rico, Mayaguez, USA

V.E. Barnes, D. Benedetti, D. Bortoletto, L. Gutay, M.K. Jha, M. Jones, K. Jung, D.H. Miller, N. Neumeister, B.C. Radburn-Smith, X. Shi, I. Shipsey, D. Silvers, J. Sun, A. Svyatkovskiy, F. Wang, W. Xie, L. Xu

Purdue University, West Lafayette, USA

N. Parashar, J. Stupak

Purdue University Calumet, Hammond, USA

A. Adair, B. Akgun, Z. Chen, K.M. Ecklund, F.J.M. Geurts, M. Guilbaud, W. Li, B. Michlin, M. Northup, B.P. Padley, R. Redjimi, J. Roberts, J. Rorie, Z. Tu, J. Zabel

Rice University, Houston, USA

B. Betchart, A. Bodek, P. de Barbaro, R. Demina, Y. Eshaq, T. Ferbel, M. Galanti, A. Garcia-Bellido, J. Han, A. Harel, O. Hindrichs, A. Khukhunaishvili, G. Petrillo, P. Tan, M. Verzetti

University of Rochester, Rochester, USA

S. Arora, A. Barker, J.P. Chou, C. Contreras-Campana, E. Contreras-Campana, D. Duggan, D. Ferencek, Y. Gershtein, R. Gray, E. Halkiadakis, D. Hidas, E. Hughes, S. Kaplan, R. Kunnawalkam Elayavalli, A. Lath, K. Nash, S. Panwalkar, M. Park, S. Salur, S. Schnetzer, D. Sheffield, S. Somalwar, R. Stone, S. Thomas, P. Thomassen, M. Walker

Rutgers, The State University of New Jersey, Piscataway, USA

M. Foerster, G. Riley, K. Rose, S. Spanier, A. York

University of Tennessee, Knoxville, USA

O. Bouhali [68], A. Castaneda Hernandez [68], M. Dalchenko, M. De Mattia, A. Delgado, S. Dildick, R. Eusebi, J. Gilmore, T. Kamon [69], V. Krutelyov, R. Mueller, I. Osipenkov, Y. Pakhotin, R. Patel, A. Perloff, A. Rose, A. Safonov, A. Tatarinov, K.A. Ulmer [2]

Texas A&M University, College Station, USA

N. Akchurin, C. Cowden, J. Damgov, C. Dragoiu, P.R. Dudero, J. Faulkner, S. Kunori, K. Lamichhane, S.W. Lee, T. Libeiro, S. Undleeb, I. Volobouev

Texas Tech University, Lubbock, USA

E. Appelt, A.G. Delannoy, S. Greene, A. Gurrola, R. Janjam, W. Johns, C. Maguire, Y. Mao, A. Melo, H. Ni, P. Sheldon, B. Snook, S. Tuo, J. Velkovska, Q. Xu

Vanderbilt University, Nashville, USA

M.W. Arenton, B. Cox, B. Francis, J. Goodell, R. Hirosky, A. Ledovskoy, H. Li, C. Lin, C. Neu, T. Sinthuprasith, X. Sun, Y. Wang, E. Wolfe, J. Wood, F. Xia

University of Virginia, Charlottesville, USA

C. Clarke, R. Harr, P.E. Karchin, C. Kottachchi Kankanamge Don, P. Lamichhane, J. Sturdy

Wayne State University, Detroit, USA

D.A. Belknap, D. Carlsmith, M. Cepeda, S. Dasu, L. Dodd, S. Duric, E. Friis, B. Gomber, M. Grothe, R. Hall-Wilton, M. Herndon, A. Hervé, P. Klabbers, A. Lanaro, A. Levine, K. Long, R. Loveless, A. Mohapatra, I. Ojalvo, T. Perry, G.A. Pierro, G. Polese, T. Ruggles, T. Sarangi, A. Savin, A. Sharma, N. Smith, W.H. Smith, D. Taylor, N. Woods

University of Wisconsin–Madison, Madison, WI, USA

† Deceased.

[1] Also at Vienna University of Technology, Vienna, Austria.

[2] Also at CERN, European Organization for Nuclear Research, Geneva, Switzerland.
[3] Also at State Key Laboratory of Nuclear Physics and Technology, Peking University, Beijing, China.
[4] Also at Institut Pluridisciplinaire Hubert Curien, Université de Strasbourg, Université de Haute Alsace Mulhouse, CNRS/IN2P3, Strasbourg, France.
[5] Also at National Institute of Chemical Physics and Biophysics, Tallinn, Estonia.
[6] Also at Skobeltsyn Institute of Nuclear Physics, Lomonosov Moscow State University, Moscow, Russia.
[7] Also at Universidade Estadual de Campinas, Campinas, Brazil.
[8] Also at Centre National de la Recherche Scientifique (CNRS) – IN2P3, Paris, France.
[9] Also at Laboratoire Leprince-Ringuet, Ecole Polytechnique, IN2P3–CNRS, Palaiseau, France.
[10] Also at Joint Institute for Nuclear Research, Dubna, Russia.
[11] Also at Helwan University, Cairo, Egypt.
[12] Now at Zewail City of Science and Technology, Zewail, Egypt.
[13] Also at Beni-Suef University, Bani Sweif, Egypt.
[14] Now at British University in Egypt, Cairo, Egypt.
[15] Now at Ain Shams University, Cairo, Egypt.
[16] Also at Université de Haute Alsace, Mulhouse, France.
[17] Also at Tbilisi State University, Tbilisi, Georgia.
[18] Also at RWTH Aachen University, III. Physikalisches Institut A, Aachen, Germany.
[19] Also at Indian Institute of Science Education and Research, Bhopal, India.
[20] Also at University of Hamburg, Hamburg, Germany.
[21] Also at Brandenburg University of Technology, Cottbus, Germany.
[22] Also at Institute of Nuclear Research ATOMKI, Debrecen, Hungary.
[23] Also at Eötvös Loránd University, Budapest, Hungary.
[24] Also at University of Debrecen, Debrecen, Hungary.
[25] Also at Wigner Research Centre for Physics, Budapest, Hungary.
[26] Also at University of Visva-Bharati, Santiniketan, India.
[27] Now at King Abdulaziz University, Jeddah, Saudi Arabia.
[28] Also at University of Ruhuna, Matara, Sri Lanka.
[29] Also at Isfahan University of Technology, Isfahan, Iran.
[30] Also at University of Tehran, Department of Engineering Science, Tehran, Iran.
[31] Also at Plasma Physics Research Center, Science and Research Branch, Islamic Azad University, Tehran, Iran.
[32] Also at Università degli Studi di Siena, Siena, Italy.
[33] Also at Purdue University, West Lafayette, USA.
[34] Also at International Islamic University of Malaysia, Kuala Lumpur, Malaysia.
[35] Also at Malaysian Nuclear Agency, MOSTI, Kajang, Malaysia.
[36] Also at Consejo Nacional de Ciencia y Tecnología, Mexico city, Mexico.
[37] Also at Warsaw University of Technology, Institute of Electronic Systems, Warsaw, Poland.
[38] Also at Institute for Nuclear Research, Moscow, Russia.
[39] Also at St. Petersburg State Polytechnical University, St. Petersburg, Russia.
[40] Also at National Research Nuclear University 'Moscow Engineering Physics Institute' (MEPhI), Moscow, Russia.
[41] Also at California Institute of Technology, Pasadena, USA.
[42] Also at Faculty of Physics, University of Belgrade, Belgrade, Serbia.
[43] Also at National Technical University of Athens, Athens, Greece.
[44] Also at Scuola Normale e Sezione dell'INFN, Pisa, Italy.
[45] Also at National and Kapodistrian University of Athens, Athens, Greece.
[46] Also at Institute for Theoretical and Experimental Physics, Moscow, Russia.
[47] Also at Albert Einstein Center for Fundamental Physics, Bern, Switzerland.
[48] Also at Gaziosmanpasa University, Tokat, Turkey.
[49] Also at Mersin University, Mersin, Turkey.
[50] Also at Cag University, Mersin, Turkey.
[51] Also at Piri Reis University, Istanbul, Turkey.
[52] Also at Adiyaman University, Adiyaman, Turkey.
[53] Also at Ozyegin University, Istanbul, Turkey.
[54] Also at Izmir Institute of Technology, Izmir, Turkey.
[55] Also at Marmara University, Istanbul, Turkey.
[56] Also at Kafkas University, Kars, Turkey.
[57] Also at Mimar Sinan University, Istanbul, Istanbul, Turkey.
[58] Also at Yildiz Technical University, Istanbul, Turkey.
[59] Also at Hacettepe University, Ankara, Turkey.
[60] Also at Rutherford Appleton Laboratory, Didcot, United Kingdom.
[61] Also at School of Physics and Astronomy, University of Southampton, Southampton, United Kingdom.
[62] Also at Instituto de Astrofísica de Canarias, La Laguna, Spain.
[63] Also at Utah Valley University, Orem, USA.
[64] Also at University of Belgrade, Faculty of Physics and Vinca Institute of Nuclear Sciences, Belgrade, Serbia.
[65] Also at Facoltà Ingegneria, Università di Roma, Roma, Italy.
[66] Also at Argonne National Laboratory, Argonne, USA.
[67] Also at Erzincan University, Erzincan, Turkey.
[68] Also at Texas A&M University at Qatar, Doha, Qatar.
[69] Also at Kyungpook National University, Daegu, Republic of Korea.